EUROPEAN ORGANIZATION FOR NUCLEAR RESEARCH

CERN–PPE/95-29

16 March 1995

Production of strange B-baryons decaying into $\Xi^{\mp}$ – $\ell^{\mp}$ pairs at LEP

DELPHI Collaboration

Abstract

An excess of events containing, in a jet, a same-sign $\Xi^{\mp} - \ell^{\mp}$ pair as compared to those with an opposite-sign $\Xi^{\mp} - \ell^{\pm}$ pair has been observed in an analysis of 1.7 million hadronic Z^0 decays collected by the DELPHI detector at LEP between 1991 and 1993 inclusive. The probability for this signal to come from non B-baryon decays is less than 5×10^{-4}. The measured production fraction corresponds to:

$$\mathcal{P}(b \to \mathrm{B-baryon}) \times \mathrm{BR}(\mathrm{B-baryon} \to \Xi^- \ \ell^- \ X) \ = \ (5.9 \pm 2.1 \pm 1.0) \times 10^{-4} \ ,$$

per lepton species, averaged for electrons and muons and assuming that the two channels have an equal contribution. Semileptonic decays of Λ_b baryons can account for less than 10% of these events and the major part of the signal has to originate from Ξ_b semileptonic decays. Using the subsample of these events where the $\Xi^{\mp}$ trajectory has been measured in the Vertex Detector, the lifetime of B-baryons producing a $\Xi^{\mp}$ in their semileptonic decay final state is found to be:

$$\tau_{\Xi_b} \ = \ 1.5^{+0.7}_{-0.4} \pm 0.3 \ ps \ .$$

(To be submitted to Zeit. f. Physik C)

P.Abreu[21], W.Adam[50], T.Adye[37], E.Agasi[31], I.Ajinenko[42], R.Aleksan[39], G.D.Alekseev[16], P.P.Allport[22], S.Almehed[24], F.M.L.Almeida[47], S.J.Alvsvaag[4], U.Amaldi[9], S.Amato[47], A.Andreazza[28], M.L.Andrieux[14], P.Antilogus[25], W-D.Apel[17], Y.Arnoud[39], B.Åsman[44], J-E.Augustin[19], A.Augustinus[31], P.Baillon[9], P.Bambade[19], F.Barao[21], R.Barate[14], G.Barbiellini[46], D.Y.Bardin[16], G.J.Barker[35], A.Baroncelli[40], O.Barring[24], J.A.Barrio[26], W.Bartl[50], M.J.Bates[37], M.Battaglia[15], M.Baubillier[23], J.Baudot[39], K-H.Becks[52], M.Begalli[6], P.Beilliere[8], Yu.Belokopytov[9], P.Beltran[11], A.C.Benvenuti[5], M.Berggren[41], D.Bertrand[2], F.Bianchi[45], M.Bigi[45], M.S.Bilenky[16], P.Billoir[23], J.Bjarne[24], D.Bloch[10], M.Blume[52], S.Blyth[35], V.Bocci[38], T.Bolognese[39], M.Bonesini[28], W.Bonivento[28], P.S.L.Booth[22], G.Borisov[42], C.Bosio[40], B.Bostjancic[43], S.Bosworth[35], O.Botner[48], B.Bouquet[19], C.Bourdarios[9], T.J.V.Bowcock[22], M.Bozzo[13], P.Branchini[40], K.D.Brand[36], R.A.Brenner[15], C.Bricman[2], L.Brillault[23], R.C.A.Brown[9], P.Bruckman[18], J-M.Brunet[8], L.Bugge[33], T.Buran[33], A.Buys[9], M.Caccia[28], M.Calvi[28], A.J.Camacho Rozas[41], T.Camporesi[9], V.Canale[38], M.Canepa[13], K.Cankocak[44], F.Cao[2], F.Carena[9], P.Carrilho[47], L.Carroll[22], C.Caso[13], V.Cassio[45], M.V.Castillo Gimenez[49], A.Cattai[9], F.R.Cavallo[5], L.Cerrito[38], V.Chabaud[9], M.Chapkin[42], Ph.Charpentier[9], L.Chaussard[25], J.Chauveau[23], P.Checchia[36], G.A.Chelkov[16], P.Chliapnikov[42], P.Chochula[7], V.Chorowicz[9], V.Cindro[43], P.Collins[9], J.L.Contreras[19], R.Contri[13], E.Cortina[49], G.Cosme[19], F.Cossutti[46], H.B.Crawley[1], D.Crennell[37], G.Crosetti[13], J.Cuevas Maestro[34], S.Czellar[15], E.Dahl-Jensen[29], J.Dahm[52], B.Dalmagne[19], M.Dam[33], G.Damgaard[29], A.Daum[17], P.D.Dauncey[37], M.Davenport[9], W.Da Silva[23], C.Defoix[8], G.Della Ricca[46], P.Delpierre[27], N.Demaria[35], A.De Angelis[9], H.De Boeck[2], W.De Boer[17], S.De Brabandere[2], C.De Clercq[2], C.De La Vaissiere[23], B.De Lotto[46], A.De Min[28], L.De Paula[47], C.De Saint-Jean[39], H.Dijkstra[9], L.Di Ciaccio[38], F.Djama[10], J.Dolbeau[8], M.Donszelmann[9], K.Doroba[51], M.Dracos[10], J.Drees[52], K.-A.Drees[52], M.Dris[32], Y.Dufour[8], F.Dupont[14], D.Edsall[1], R.Ehret[17], G.Eigen[4], T.Ekelof[48], G.Ekspong[44], M.Elsing[52], J-P.Engel[10], N.Ershaidat[23], M.Espirito Santo[21], D.Fassouliotis[32], M.Feindt[9], A.Fenyuk[42], A.Ferrer[49], T.A.Filippas[32], A.Firestone[1], H.Foeth[9], E.Fokitis[32], F.Fontanelli[13], F.Formenti[9], B.Franek[37], P.Frenkiel[8], D.C.Fries[17], A.G.Frodesen[4], R.Fruhwirth[50], F.Fulda-Quenzer[19], H.Furstenau[9], J.Fuster[49], D.Gamba[45], M.Gandelman[6], C.Garcia[49], J.Garcia[41], C.Gaspar[9], U.Gasparini[36], Ph.Gavillet[9], E.N.Gazis[32], D.Gele[10], J-P.Gerber[10], D.Gillespie[9], R.Gokieli[51], B.Golob[43], G.Gopal[37], L.Gorn[1], M.Gorski[51], V.Gracco[13], F.Grard[2], E.Graziani[40], G.Grosdidier[19], P.Gunnarsson[44], M.Gunther[48], J.Guy[37], U.Haedinger[17], F.Hahn[52], M.Hahn[17], S.Hahn[52], S.Haider[31], Z.Hajduk[18], A.Hakansson[24], A.Hallgren[48], K.Hamacher[52], W.Hao[31], F.J.Harris[35], V.Hedberg[24], R.Henriques[21], J.J.Hernandez[49], P.Herquet[2], H.Herr[9], T.L.Hessing[9], E.Higon[49], H.J.Hilke[9], T.S.Hill[1], S-O.Holmgren[44], P.J.Holt[35], D.Holthuizen[31], M.Houlden[22], J.Hrubec[50], K.Huet[2], K.Hultqvist[44], P.Ioannou[3], J.N.Jackson[22], R.Jacobsson[44], P.Jalocha[18], R.Janik[7], G.Jarlskog[24], P.Jarry[39], B.Jean-Marie[19], E.K.Johansson[44], L.Jonsson[24], C.Joram[9], P.Juillot[10], M.Kaiser[17], G.Kalmus[37], F.Kapusta[23], M.Karlsson[44], E.Karvelas[11], S.Katsanevas[3], E.C.Katsoufis[32], R.Keranen[15], B.A.Khomenko[16], N.N.Khovanski[16], B.King[22], N.J.Kjaer[29], H.Klein[9], A.Klovning[4], P.Kluit[31], J.H.Koehne[17], B.Koene[31], P.Kokkinias[11], M.Koratzinos[9], V.Kostioukhine[42], C.Kourkoumelis[3], O.Kouznetsov[13], P.-H.Kramer[52], M.Krammer[50], C.Kreuter[17], J.Krolikowski[51], I.Kronkvist[24], Z.Krumstein[16], W.Krupinski[18], P.Kubinec[7], W.Kucewicz[18], K.Kurvinen[15], C.Lacasta[49], I.Laktineh[25], S.Lamblot[23], C.Lambropoulos[11], J.W.Lamsa[1], L.Lanceri[46], D.W.Lane[1], P.Langefeld[52], V.Lapin[42], I.Last[22], J-P.Laugier[39], R.Lauhakangas[15], G.Leder[50], F.Ledroit[14], V.Lefebure[2], C.K.Legan[1], R.Leitner[30], Y.Lemoigne[39], J.Lemonne[2], G.Lenzen[52], V.Lepeltier[19], T.Lesiak[36], D.Liko[50], R.Lindner[52], A.Lipniacka[19], I.Lippi[36], B.Loerstad[24], M.Lokajicek[12], J.G.Loken[35], J.M.Lopez[41], A.Lopez-Fernandez[9], M.A.Lopez Aguera[41], D.Loukas[11], P.Lutz[39], L.Lyons[35], J.MacNaughton[50], G.Maehlum[17], A.Maio[21], A.Maltezos[11], V.Malychev[16], F.Mandl[50], J.Marco[41], B.Marechal[47], M.Margoni[36], J-C.Marin[9], C.Mariotti[40], A.Markou[11], T.Maron[52], C.Martinez-Rivero[41], F.Martinez-Vidal[49], S.Marti i Garcia[49], F.Matorras[41], C.Matteuzzi[28], G.Matthiae[38], M.Mazzucato[36], M.Mc Cubbin[9], R.Mc Kay[1], R.Mc Nulty[22], J.Medbo[48], C.Meroni[28], W.T.Meyer[1], M.Michelotto[36], E.Migliore[45], L.Mirabito[25], W.A.Mitaroff[50], U.Mjoernmark[24], T.Moa[44], R.Moeller[29], K.Moenig[9], M.R.Monge[13], P.Morettini[13], H.Mueller[17], L.M.Mundim[6], W.J.Murray[37], B.Muryn[18], G.Myatt[35], F.Naraghi[14], F.L.Navarria[5], S.Navas[49], P.Negri[28], S.Nemecek[12], W.Neumann[52], N.Neumeister[50], R.Nicolaidou[3], B.S.Nielsen[29], V.Nikolaenko[10], P.Niss[44], A.Nomerotski[36], A.Normand[35], W.Oberschulte-Beckmann[17], V.Obraztsov[42], A.G.Olshevski[16], A.Onofre[21], R.Orava[15], A.Ostankov[42], K.Osterberg[15], A.Ouraou[39], P.Paganini[19], M.Paganoni[28], P.Pages[10], H.Palka[18], Th.D.Papadopoulou[32], L.Pape[9], F.Parodi[13], A.Passeri[40], M.Pegoraro[36], J.Pennanen[15], L.Peralta[21], M.Pernicka[50], A.Perrotta[5], C.Petridou[46], A.Petrolini[13], H.T.Phillips[37], G.Piana[13], F.Pierre[39], M.Pimenta[21], S.Plaszczynski[19], O.Podobrin[17], M.E.Pol[6], G.Polok[18], P.Poropat[46], V.Pozdniakov[16], M.Prest[46], P.Privitera[38], A.Pullia[28], D.Radojicic[35], S.Ragazzi[28], H.Rahmani[32], J.Rames[12], P.N.Ratoff[20], A.L.Read[33], M.Reale[52], P.Rebecchi[19], N.G.Redaelli[28], M.Regler[50], D.Reid[9], P.B.Renton[35], L.K.Resvanis[3], F.Richard[19], J.Richardson[22], J.Ridky[12], G.Rinaudo[45], I.Ripp[39], A.Romero[45], I.Roncagliolo[13], P.Ronchese[36], L.Roos[14], E.I.Rosenberg[1], E.Rosso[9], P.Roudeau[19], T.Rovelli[5], W.Ruckstuhl[31], V.Ruhlmann-Kleider[39], A.Ruiz[41], K.Rybicki[18], H.Saarikko[15], Y.Sacquin[39], A.Sadovsky[16], G.Sajot[14], J.Salt[49], J.Sanchez[26], M.Sannino[13], H.Schneider[17], M.A.E.Schyns[52], G.Sciolla[45], F.Scuri[46], Y.Sedykh[16], A.M.Segar[35], A.Seitz[17], R.Sekulin[37], R.C.Shellard[6], I.Siccama[31], P.Siegrist[39], S.Simonetti[39], F.Simonetto[36], A.N.Sisakian[16], B.Sitar[7], T.B.Skaali[33], G.Smadja[25], N.Smirnov[42], O.Smirnova[16], G.R.Smith[37], R.Sosnowski[51], D.Souza-Santos[6], T.Spassov[21], E.Spiriti[40], S.Squarcia[13], H.Staeck[52], C.Stanescu[40], S.Stapnes[33], I.Stavitski[36], G.Stavropoulos[11], K.Stepaniak[51], F.Stichelbaut[9], A.Stocchi[19], J.Strauss[50], R.Strub[10], B.Stugu[4], M.Szczekowski[51], M.Szeptycka[51], T.Tabarelli[28],

J.P.Tavernet[23], O.Tchikilev[42], G.E.Theodosiou[11], A.Tilquin[27], J.Timmermans[31], L.G.Tkatchev[16], T.Todorov[10], D.Z.Toet[31], A.Tomaradze[2], E.Torassa[45], L.Tortora[40], G.Transtromer[24], D.Treille[9], W.Trischuk[9], G.Tristram[8], A.Trombini[19], C.Troncon[28], A.Tsirou[9], M-L.Turluer[39], I.A.Tyapkin[16], M.Tyndel[37], S.Tzamarias[22], B.Ueberschaer[52], S.Ueberschaer[52], O.Ullaland[9], V.Uvarov[42], G.Valenti[5], E.Vallazza[9], C.Vander Velde[2], G.W.Van Apeldoorn[31], P.Van Dam[31], W.K.Van Doninck[2], J.Van Eldik[31], G.Vegni[28], L.Ventura[36], W.Venus[37], F.Verbeure[2], M.Verlato[36], L.S.Vertogradov[16], D.Vilanova[39], P.Vincent[25], L.Vitale[46], E.Vlasov[42], A.S.Vodopyanov[16], M.Voutilainen[15], V.Vrba[12], H.Wahlen[52], C.Walck[44], A.Wehr[52], M.Weierstall[52], P.Weilhammer[9], A.M.Wetherell[9], D.Wicke[52], J.H.Wickens[2], M.Wielers[17], G.R.Wilkinson[35], W.S.C.Williams[35], M.Winter[10], M.Witek[9], G.Wormser[19], K.Woschnagg[48], K.Yip[35], L.Yu[35], F.Zach[25], A.Zaitsev[42], A.Zalewska[18], P.Zalewski[51], D.Zavrtanik[43], E.Zevgolatakos[11], N.I.Zimin[16], M.Zito[39], D.Zontar[43], R.Zuberi[35], G.C.Zucchelli[44], G.Zumerle[36]

[1] Ames Laboratory and Department of Physics, Iowa State University, Ames IA 50011, USA
[2] Physics Department, Univ. Instelling Antwerpen, Universiteitsplein 1, B-2610 Wilrijk, Belgium
and IIHE, ULB-VUB, Pleinlaan 2, B-1050 Brussels, Belgium
and Faculté des Sciences, Univ. de l'Etat Mons, Av. Maistriau 19, B-7000 Mons, Belgium
[3] Physics Laboratory, University of Athens, Solonos Str. 104, GR-10680 Athens, Greece
[4] Department of Physics, University of Bergen, Allégaten 55, N-5007 Bergen, Norway
[5] Dipartimento di Fisica, Università di Bologna and INFN, Via Irnerio 46, I-40126 Bologna, Italy
[6] Centro Brasileiro de Pesquisas Físicas, rua Xavier Sigaud 150, RJ-22290 Rio de Janeiro, Brazil
and Depto. de Física, Pont. Univ. Católica, C.P. 38071 RJ-22453 Rio de Janeiro, Brazil
and Inst. de Física, Univ. Estadual do Rio de Janeiro, rua São Francisco Xavier 524, Rio de Janeiro, Brazil
[7] Comenius University, Faculty of Mathematics and Physics, Mlynska Dolina, SK-84215 Bratislava, Slovakia
[8] Collège de France, Lab. de Physique Corpusculaire, IN2P3-CNRS, F-75231 Paris Cedex 05, France
[9] CERN, CH-1211 Geneva 23, Switzerland
[10] Centre de Recherche Nucléaire, IN2P3 - CNRS/ULP - BP20, F-67037 Strasbourg Cedex, France
[11] Institute of Nuclear Physics, N.C.S.R. Demokritos, P.O. Box 60228, GR-15310 Athens, Greece
[12] FZU, Inst. of Physics of the C.A.S. High Energy Physics Division, Na Slovance 2, 180 40, Praha 8, Czech Republic
[13] Dipartimento di Fisica, Università di Genova and INFN, Via Dodecaneso 33, I-16146 Genova, Italy
[14] Institut des Sciences Nucléaires, IN2P3-CNRS, Université de Grenoble 1, F-38026 Grenoble Cedex, France
[15] Research Institute for High Energy Physics, SEFT, P.O. Box 9, FIN-00014 Helsinki, Finland
[16] Joint Institute for Nuclear Research, Dubna, Head Post Office, P.O. Box 79, 101 000 Moscow, Russian Federation
[17] Institut für Experimentelle Kernphysik, Universität Karlsruhe, Postfach 6980, D-76128 Karlsruhe, Germany
[18] High Energy Physics Laboratory, Institute of Nuclear Physics, Ul. Kawiory 26a, PL-30055 Krakow 30, Poland
[19] Université de Paris-Sud, Lab. de l'Accélérateur Linéaire, IN2P3-CNRS, Bat 200, F-91405 Orsay Cedex, France
[20] School of Physics and Materials, University of Lancaster, Lancaster LA1 4YB, UK
[21] LIP, IST, FCUL - Av. Elias Garcia, 14-1^{o}, P-1000 Lisboa Codex, Portugal
[22] Department of Physics, University of Liverpool, P.O. Box 147, Liverpool L69 3BX, UK
[23] LPNHE, IN2P3-CNRS, Universités Paris VI et VII, Tour 33 (RdC), 4 place Jussieu, F-75252 Paris Cedex 05, France
[24] Department of Physics, University of Lund, Sölvegatan 14, S-22363 Lund, Sweden
[25] Université Claude Bernard de Lyon, IPNL, IN2P3-CNRS, F-69622 Villeurbanne Cedex, France
[26] Universidad Complutense, Avda. Complutense s/n, E-28040 Madrid, Spain
[27] Univ. d'Aix - Marseille II - CPP, IN2P3-CNRS, F-13288 Marseille Cedex 09, France
[28] Dipartimento di Fisica, Università di Milano and INFN, Via Celoria 16, I-20133 Milan, Italy
[29] Niels Bohr Institute, Blegdamsvej 17, DK-2100 Copenhagen 0, Denmark
[30] NC, Nuclear Centre of MFF, Charles University, Areal MFF, V Holesovickach 2, 180 00, Praha 8, Czech Republic
[31] NIKHEF-H, Postbus 41882, NL-1009 DB Amsterdam, The Netherlands
[32] National Technical University, Physics Department, Zografou Campus, GR-15773 Athens, Greece
[33] Physics Department, University of Oslo, Blindern, N-1000 Oslo 3, Norway
[34] Dpto. Fisica, Univ. Oviedo, C/P. Pérez Casas, S/N-33006 Oviedo, Spain
[35] Department of Physics, University of Oxford, Keble Road, Oxford OX1 3RH, UK
[36] Dipartimento di Fisica, Università di Padova and INFN, Via Marzolo 8, I-35131 Padua, Italy
[37] Rutherford Appleton Laboratory, Chilton, Didcot OX11 OQX, UK
[38] Dipartimento di Fisica, Università di Roma II and INFN, Tor Vergata, I-00173 Rome, Italy
[39] Centre d'Etude de Saclay, DSM/DAPNIA, F-91191 Gif-sur-Yvette Cedex, France
[40] Istituto Superiore di Sanità, Ist. Naz. di Fisica Nucl. (INFN), Viale Regina Elena 299, I-00161 Rome, Italy
[41] C.E.A.F.M., C.S.I.C. - Univ. Cantabria, Avda. los Castros, S/N-39006 Santander, Spain, (CICYT-AEN93-0832)
[42] Inst. for High Energy Physics, Serpukov P.O. Box 35, Protvino, (Moscow Region), Russian Federation
[43] J. Stefan Institute and Department of Physics, University of Ljubljana, Jamova 39, SI-61000 Ljubljana, Slovenia
[44] Fysikum, Stockholm University, Box 6730, S-113 85 Stockholm, Sweden
[45] Dipartimento di Fisica Sperimentale, Università di Torino and INFN, Via P. Giuria 1, I-10125 Turin, Italy
[46] Dipartimento di Fisica, Università di Trieste and INFN, Via A. Valerio 2, I-34127 Trieste, Italy
and Istituto di Fisica, Università di Udine, I-33100 Udine, Italy
[47] Univ. Federal do Rio de Janeiro, C.P. 68528 Cidade Univ., Ilha do Fundão BR-21945-970 Rio de Janeiro, Brazil
[48] Department of Radiation Sciences, University of Uppsala, P.O. Box 535, S-751 21 Uppsala, Sweden
[49] IFIC, Valencia-CSIC, and D.F.A.M.N., U. de Valencia, Avda. Dr. Moliner 50, E-46100 Burjassot (Valencia), Spain
[50] Institut für Hochenergiephysik, Österr. Akad. d. Wissensch., Nikolsdorfergasse 18, A-1050 Vienna, Austria
[51] Inst. Nuclear Studies and University of Warsaw, Ul. Hoza 69, PL-00681 Warsaw, Poland
[52] Fachbereich Physik, University of Wuppertal, Postfach 100 127, D-42097 Wuppertal 1, Germany

1 Introduction

In addition to the Λ_b^0(bud), quark models predict the existence of three beauty baryonic states[†] which are expected to decay through the weak interaction: the Ξ_b^0(bsu), the Ξ_b^-(bsd) and the Ω_b^-(bss). These states have not yet been observed. The other non-strange B-baryon resonances of spin 1/2 and 3/2 like the Σ_b and the Σ_b^* must decay by strong interaction to the Λ_b^0 [1]. The equivalent excited strange B-baryon states, the Ξ_b' and the Ξ_b^*, are expected to decay by strong or electromagnetic interactions to Ξ_b states.

Baryon production in jets is generally viewed as the fusion between a quark and a diquark. When diquark-antidiquark pairs are produced during the hadronization of the jets, they will rarely contain a heavy quark. As the heavy quark is therefore always a primary parton, the production of heavy baryons in jets may originate from more fundamental mechanisms than the production of baryons made with light quarks only. It is thus of interest to study these mechanisms.

In the semileptonic decays of heavy hadrons, the flavour(s) of the light spectator system contained in the initial state is(are) transmitted to the final state. This property has been used previously to isolate different species of B hadrons. The reconstruction of a lepton produced at large transverse momentum relative to the jet axis, accompanied by a D_s meson of opposite electric charge, allows the selection [2] of pure samples of B_s^0 mesons[‡]. In the same way, the excess of events containing a Λ^0 accompanied by a negative lepton, as compared to those accompanied by a positive lepton, gives a measurement of Λ_b production [3].

Following the same idea, the production rates of $\Xi^\mp$ accompanied by a lepton of same or opposite charge, in the same jet, are compared in this paper. Because of the strangeness content of $\Xi^\mp$ hyperons, this can be a way to identify the production of Ξ_b baryons. In the following, same-sign $\Xi^\mp - \ell^\mp$ pairs will be called $right-sign$ pairs because the signal from B-baryon decays is expected in these events; opposite-sign pairs will be called $wrong-sign$ pairs.

This paper describes the first experimental observation of $\Xi^\mp - \ell^\mp$ pairs from the semileptonic decays of B-baryons and discusses the interpretation of these events in terms of Ξ_b baryon production. It is organized in the following way, detector components of importance in this analysis are described in section 2. Section 3 describes the lepton identification in DELPHI. Algorithms for $\Xi^\mp$ reconstruction are described in section 4. In section 5, the mechanisms giving rise to the desired topology are listed and the characteristics which allow one to isolate this final state are given in section 6. Section 7 gives the evidence for a signal of Ξ_b baryon semileptonic decays. Measurements of the production rate and lifetime of these events are described in section 8 and 9 respectively.

2 Detector description and event selection

A complete description of the DELPHI apparatus is given in [4]. Only components of the DELPHI detector which play an important role in the present analysis are described here.

The muon detector is a set of drift chambers (each with 2 layers) providing three-dimensional information. In the barrel part three sets of chambers, the first located inside the magnet return yoke and the other two outside, cover polar angles between 52° and 128°. The third set, which completes the azimuthal coverage, has a small overlap

[†] Heavier baryons containing two or more heavy quarks are not considered in this analysis.

[‡] Otherwise explicitly stated, charged conjugate states are always implied.

with the others. Two sets of forward muon chambers cover polar angles from 9° to 43° and 137° to 171°. In each arm the first set is located inside the yoke and the second outside.

The barrel electromagnetic calorimeter (HPC) covers the polar region 45° to 135°.

The central tracking system, comprising the inner detector (ID), the time projection chamber (TPC) and the outer detector (OD), measures charged particles with polar angles between 30° and 150° with a resolution of $\sigma(p)/p \simeq 0.0013 \times p$ (p in units of GeV/c). The TPC, the main tracking device, is a cylinder of 30 cm inner radius, 122 cm outer radius and 2.7 m length. For polar angles between 39° and 141° it provides up to 16 space points along the charged particle trajectory.

The Vertex Detector (VD) [5] is very important in this analysis. It is made of three concentric shells of Si-strip detectors at radii of 6.3, 9 and 11 cm covering the central region between 43° and 137°. The shells surround the beryllium beam pipe of internal radius 5.3 cm and wall thickness 1.45 mm. Each shell consists of 24 modules with about 10 % overlap in azimuth between the modules. Each module holds 4 detectors with strips parallel to the beam direction. The silicon detectors are 300 μm thick and have a diode pitch of 25 μm. The read-out strips (50 μm pitch) are AC-coupled and give a 5 μm intrinsic precision on the coordinates of the charged particle tracks, transverse to the beam direction.

Hadronic Z^0 decays have been isolated from all registered events by applying standard selection criteria [7]. Correcting for the 5% losses induced by these cuts, the sample amounts to 1.7 million hadronic Z^0 decays which have been registered by DELPHI from 1991 to 1993.

Simulated events have been produced using the Lund parton shower model in the JETSET 7.3 program[8] with parameters optimized by DELPHI, passed through the DELphi detector SIMulation, DELSIM [9] and processed with the same event reconstruction as the data. The samples are described in section 7.

3 Lepton identification

Muons are identified by combining the muon chamber hits with the tracking information. The tracks of charged particles are extrapolated to the muon chambers and then associated and fitted to the hits. Information from the muon chambers alone allows a measurement of the position and direction of a track element. These are then compared to the corresponding parameters of the extrapolated track and a χ^2 test is used to determine the association of the track with the muon chamber hits.

The electron candidates are identified by combining the electromagnetic shower information from the HPC with the particle ionization loss, dE/dx, measured by the TPC. A sizeable fraction of electrons come from photon conversion. They are partially rejected if two oppositely charged particles form a secondary vertex where the invariant mass is zero within measurement errors.

	$\mathcal{P}(\ l \to l\ )\%$	$\mathcal{P}(\ h \to l\ )\%$
muon	85.0 ± 1.0	0.99 ± 0.15
electron	53.7 ± 1.2	0.6 ± 0.2

Table 1: Probabilities of lepton identification for real leptons and for hadrons.

The global identification efficiencies for muons and electrons with momenta larger than 3 GeV/c, and the corresponding probabilities for a hadron to be misidentified as a lepton, are given in Table 1. These values have been obtained using the detailed simulation code of the DELPHI detector, DELSIM [9], and have been checked on real data using selected events samples such as $K^0_s \to \pi^+\pi^-$, $Z^0 \to \mu^+\mu^-$, converted photons before the HPC, $\gamma\gamma \to \ell^+\ell^-$ and hadronic τ decays [6].

4 Reconstruction of $\Xi^\mp$ hyperons

The two algorithms which have been used to reconstruct the decay of a cascade hyperon:

$$\begin{aligned} \Xi^- &\to \Lambda\, \pi^- \\ &\hookrightarrow p\, \pi^- \end{aligned}$$

are described in sections 4.1 and 4.2.

4.1 The $\Xi^\mp$ trajectory is measured in the VD

The first method, called "HT" (Hyperon Tracking) in the following, applies to decays that occur after the last layer of the VD. Due to their large lifetimes, charged hyperons are often seen in the three layers of the VD. For a $\Xi^\mp$ of 5 GeV energy, the probability that it decays after the VD outer layer is larger than 50%. Most such particles will not travel far enough into the main tracking detector, the TPC, to be reconstructed, and in this case the VD hits cannot be associated to tracks reconstructed in the event. A $\Xi^\mp$ track candidate is defined as a set of 3 hits in the VD, not associated to any track, pointing towards the main interaction vertex. In this way, only relatively energetic hyperons are kept. The soft pion produced in the $\Xi^\mp$ decay is searched for in the central tracking system and the $\Xi^\mp$ decay vertex is obtained using the $\Xi^\mp$ and the pion trajectories. The Λ^0 decay position is searched for inside a cone, whose point is located at the $\Xi^\mp$ decay vertex, the axis of which is the direction of flight of the $\Xi^\mp$. The pion candidate from the Λ decay must have a momentum between 0.1 and 3 GeV/c with an impact parameter larger than 2.5 mm relative to the event main vertex; the momentum of the proton candidate has to be larger than 1 GeV/c. The χ^2 probability that the proton and pion make a vertex has to be larger than 1% with the mass of the $p-\pi$ system constrained to the Λ mass. Finally, the Ξ , π and Λ are required to form a common vertex and to satisfy the constraints on momentum conservation with a χ^2 probability larger than 1%. The efficiency of this algorithm has been measured using simulation and found to be (2.0 ± 0.1)% for $\Xi^\mp$ momenta larger than 3 GeV/c. This number includes the branching fraction of the $\Lambda^0 \to\ p\ \pi$ channel (66 %), the limited solid angle covered by the VD ($\simeq$ 73 %), the various track reconstruction efficiencies and the correction to account for differences in the efficiency of the VD between data and the simulation.

From a sample of 1.7 million hadronic Z^0 decays, 548 ± 36 $\Xi^\mp$ have been reconstructed, within an interval of $\pm$ 10MeV/c^2 centered on the nominal $\Xi^\mp$ mass (1321.3 MeV/c^2) [11]; the $\Lambda\ \pi$ mass distribution is shown in Fig. 1.a. The fitted mass and width of the signal are respectively 1321.2 ± 0.2 MeV/c^2 and 7.8 ± 0.6 MeV/c^2. These values have been obtained by fitting a Breit-Wigner distribution to account for the signal and a first order polynomial for the background. The algorithm isolates the $\Xi^\mp$ sample with a purity of (92 ± 3)%. As the $\Xi^\mp$ track is measured in the VD, these events can also be used to search for secondary vertices from heavy flavour decays.

4.2 Only $\Xi^{\mp}$ decay products are measured

The second method, referred to as "$\Lambda\pi$", is more traditional in its approach. The Λ^0 is reconstructed first and is combined with a charged pion of appropriate electric charge. The candidate proton from the Λ^0 decay must have a momentum larger than 0.5 GeV/c and the associated pion candidate a momentum larger than 0.1 GeV/c. The impact parameter of the pion relative to the primary vertex, measured in the plane transverse to the beam direction, has to be larger than two times its measurement error. The same selection criteria have been applied to the corresponding parameters of the candidate pion from the $\Xi^{\mp}$ decay. The vertex fits at the Λ^0 and $\Xi^{\mp}$ decay vertices must have a χ^2 probability larger than 1%. It is also required that the $\Xi^{\mp}$ hyperon decay vertex be at least 1 cm in the transverse plane (and the Λ^0 decay vertex be at least 2 cm), from the primary vertex. The efficiency of this second algorithm for $\Xi^{\mp}$ particles of momentum larger than 3 GeV/c, including branching ratios and solid angle acceptances as in section 4.1, is (7.0 ± 0.1)% and 2175 ± 97 have been reconstructed (Fig. 1.b).

The inclusive production rate of the $\Xi^{\mp}$ has been measured using the "$\Lambda\pi$" algorithm:

$$N((\Xi^- + \bar{\Xi}^+)/Z^0 \rightarrow \text{hadrons}) \;=\; 0.0257 \pm 0.0012(\text{stat.}) \pm 0.0020(\text{syst.}).$$

and found to be in agreement with previously published results [10].

The main source of systematic uncertainty comes from the use of the simulation to account for the fraction of the momentum distribution, below 2 GeV/c, for which there is no acceptance in this analysis. An uncertainty of 30% has been assumed on this correction. The momentum distribution of the reconstructed $\Xi^{\mp}$ agrees with the expectations from the simulation, and the measured mean decay length, 4.8 ± 0.4 cm, agrees with published results (4.91 cm)[11]. From the number of $\Xi^{\mp}$ reconstructed using the "$\Lambda\pi$" algorithm and the efficiencies of the two algorithms one expects 621 ± 42 $\Xi^{\mp}$ from the "HT" algorithm: this value agrees with the number quoted in section 4.1 showing that the relative efficiency between the two algorithms is acceptable.

The overall $\Xi^{\mp}$ reconstruction efficiency, for particles of momentum larger than 3 GeV/c found by either or both of the two algorithms is:

$$\epsilon(\Xi^{\mp}) \;=\; (8.3 \;\pm\; 0.2)\%$$

5 Possible sources of $\Xi^{\mp} - \ell$ pairs in the same jet

The different mechanisms contributing to the production of a $\Xi^{\mp} - \ell$ pair in the same jet are reviewed. As mentioned in the introduction, B-baryon direct semileptonic decays contribute mainly to right-sign pairs. It is shown that, on quite general grounds, one expects an excess of events in the wrong-sign pair sample from all other mechanisms. The expected number of events from the simulation, are given in section 7 for heavy baryon semileptonic decays. In the final analysis, direct semileptonic decays of B hadrons have been selected by requiring that the lepton transverse momentum, measured relative to the direction of the jet, after having removed the lepton from it, be larger than 1 GeV/c. Possible sources of background have to be envisaged mainly in this domain.

Two main classes of events are considered, depending on the origin of the $\Xi^{\mp}$ hyperon.

5.1 $\Xi^{\mp}$ hyperons from decays

Leptons from weak decays are produced at secondary vertices, whereas misidentified hadrons can come also from the event primary vertex.

Only heavy flavour baryon semileptonic decays contribute events with a Ξ^- and with the lepton produced by semileptonic decay of a heavy hadron. Semileptonic B meson decays can be neglected because, due to the small available phase space, the lepton momentum, in the B centre of mass system, is lower than 1 GeV/c.

- Strange B-baryons:
  The two Ξ_b baryonic states are expected to decay in the following way (Fig. 2.a):

$$\begin{array}{rcl} \Xi_b^- & \rightarrow & \Xi_c^0\ \ell^-\ \bar{\nu}_l\ X \\ & & \hookrightarrow\ \Xi^-\ X' \end{array} \quad , \quad \begin{array}{rcl} \Xi_b^0 & \rightarrow & \Xi_c^+\ \ell^-\ \bar{\nu}_l\ X\ . \\ & & \hookrightarrow\ \Xi^-\ X' \end{array}$$

  As the production of excited Ξ_c states in the semileptonic decays of Ξ_b baryons will mainly give a Ξ_c state, the production rate of $\Xi^\mp - \ell^\mp$ is proportional to the inclusive semileptonic branching fraction of Ξ_b baryons times the inclusive branching fraction of Ξ_c baryons to Ξ^- hyperons. In the simulation, the probability to obtain a $\Xi^-\ \ell^-$ from a direct Ξ_b baryon semileptonic decay, in a b jet is:

$$\begin{array}{lcll} \mathcal{P}(b \rightarrow \Xi_b \rightarrow \Xi^-\ \ell^-\ X) & = & \mathcal{P}(b \rightarrow \Xi_b) & (\ 1\ \%\ \text{for}\ \Xi_b^0\ +\ \Xi_b^-\ \text{states}\ ) \\ & \times & \mathcal{P}(\Xi_b \rightarrow \Xi_c\ \ell^-\ X) & (\ 10\ \%\ \text{for}\ \ell = \text{e or}\ \mu\ ) \\ & \times & \mathcal{P}(\Xi_c \rightarrow \Xi^-\ X) & (\ 17\ \%\ \Xi_c^+\ \text{and}\ \Xi_c^0\ \text{average}\ ) \\ & = & 1.7\ 10^{-4}\ . & \end{array} \qquad (1)$$

  It has been assumed that the semileptonic branching fraction of heavy hadrons into an electron or a muon is the same and the notation l refers to only one of the lepton categories. Semileptonic decays with emission of a τ lepton are assumed to be relatively suppressed and are not considered.
  The value of the semileptonic branching fraction is a reasonable assumption because similar values are expected for all B hadrons, but the two other quantities are largely uncertain and have still to be determined by experiments.
- Λ_b semileptonic decays
  A much larger contribution to the $\Xi^\mp\ -\ \ell^\mp$ final state is expected from Ξ_b baryons than from Λ_b^0 states, even if their initial production rate is smaller. Semileptonic decays of Λ_b^0 (Fig. 2.b) can contribute to $\Xi^\mp\ -\ \ell^\mp$ candidates through the decay chain:

$$\begin{array}{rcl} \Lambda_b^0 & \rightarrow & \Lambda_c^+\ \ell^-\ \bar{\nu}_l\ X\ . \\ & & \hookrightarrow\ \Xi^-\ K^+\ \pi^+ \end{array}$$

  The branching ratio for this decay of the Λ_c was measured by the CLEO collaboration [14] to be $(\ 0.34 \pm 0.13\ )\%$ assuming $\text{BR}(\Lambda_c \rightarrow pK^-\pi^+)\ = (\ 4.3 \pm 1.0 \pm 0.8\ )\%$ [15]. It has been measured also by CLEO [14] that $(\ 42 \pm 12\ )\%$ of the $\Lambda_c \rightarrow \Xi^- K^+ \pi^+$ decays were due to the two-body decay $\Lambda_c \rightarrow \Xi^{*0} K^+$ which has a branching fraction of $(\ 0.23 \pm 0.11\ )\%$. Other possibilities to produce a Ξ^- in a Λ_c^+ decay require the production of at least an additional pion. Because of the very small Q value of these decays, the contribution from such configurations should not exceed the previous one unless they are favoured dynamically by the production of resonances in the final state. These effects, which can produce enhancement factors of two to three times on the decay rates, as observed in D decays, are unlikely in this case because there is not enough available phase-space to produce a ρ^+ or a K^* at its pole mass value.

A large effect from Ξ^* states is also unlikely because Ξ^* contributes only to about 50% of the $\Xi^- K^+ \pi^+$ as noticed previously. In the simulation the production of $\Xi^\mp$ from Λ_b decays amount to 0.3%, a value which is consistent with the expected contribution from the decay $\Lambda_c^+ \to \Xi^- K^+ \pi^+$ alone, and the probability to have this final state in a b quark jet is:

$$\begin{aligned} \mathcal{P}(b \to \Lambda_b^0 \to \Xi^- \ \ell^- \ X) &= \mathcal{P}(b \to \Lambda_b^0) && (\ 7.8\ \%\ ) \\ &\times \mathcal{P}(\Lambda_b^0 \to \Lambda_c \ \ell^- \ X) && (\ 10\ \%\ \text{for}\ \ell = \text{e or}\ \mu\ ) \\ &\times \mathcal{P}(\Lambda_c \to \Xi^- \ X) && (\ 3.\ 10^{-3}\ ) \\ &= 2.3\ 10^{-5}\ . \end{aligned} \tag{2}$$

Direct semileptonic decays of a Λ_b with a Ξ_c and a kaon produced in the accompanying system (Fig. 2.c) are expected to be negligible (as in the search for the B_s^0 meson using the $D_s - \ell$ final state, where semileptonic decays with a D_s and a kaon in the final state, from non-strange B hadrons could be neglected [2]).

- Strange charmed baryons
  Semileptonic decays of Ξ_c baryons (Fig. 2.d) give wrong-sign $\Xi^\mp - \ell^\pm$ pairs with a lepton emitted at low transverse momentum. The absolute contribution from this channel is expected to be small because Ξ_c^+ states will produce rather few Ξ^- when they decay semileptonically and also because the Ξ_c^0 states, having a very short lifetime, are expected to have a correspondingly small semileptonic branching fraction:

$$\begin{aligned} \mathcal{P}(c \to \Xi_c \to \Xi^- \ell^+ X) &\simeq \mathcal{P}(c \to \Xi_c^0) && (\ 0.5\ \%\ ) \\ &\times \mathcal{P}(\Xi_c^0 \to \Xi^- \ell^+ X) && (1.3\ \%) \\ &= 6.5 \times 10^{-5}\ . \end{aligned} \tag{3}$$

  For the first number, it has been assumed that the probability to produce strange, charmed or beauty baryons is the same (1%) but only the Ξ_c^0 state is expected to contribute to the $\Xi^\mp - \ell$ final state. The second number is the product of the expected Ξ_c^0 semileptonic branching fraction (1.8 %) times the probability for Ξ^- production in such decays, taken from the simulation.
- Fake leptons
  The contribution from fake leptons with a P_t larger than 1 GeV/c is negligible relative to other sources and should give rise to similar numbers of right-sign and of wrong-sign $\Xi^\mp - \ell^\pm$ pairs.

5.2 $\Xi^\mp$ hyperons from fragmentation

Ξ^- are produced during the hadronization of the quark jets and are a source of background. They require the emission of an $s - \bar{s}$ quark pair and of a diquark-antidiquark pair containing at least one strange quark. As the $\Xi^\mp$ and the lepton both are required to have a momentum larger than 3 GeV/c, it is probable that the $\Xi^\mp$ and the hadron producing the lepton are close in rapidity, and therefore only those cases will be dealt with in the qualitative description given below. The expected contribution from these mechanisms, as the JETSET simulation predicts them will be given in section 7.

Several mechanisms contribute to the $\Xi - \ell$ final state depending on the origin of the lepton.

- The lepton originates from the direct semileptonic decay of a B-baryon (Fig. 3.a): this is a source of wrong-sign $\Xi^{\mp} - \ell^{\pm}$ pairs. The contribution from Λ_b^0 is expected to be similar or even smaller than that from the Ξ_b baryonic states.
- The lepton originates from the direct semileptonic decay of a B meson (Fig. 3.b, c, d): when the lepton comes from a $\bar{B}_s^0$ semileptonic decay, the Ξ^- can share the same $s - \bar{s}$ pair with the $\bar{B}_s^0$ meson and then be quite energetic (Fig. 3.b). As the $\bar{B}_s^0$ meson is expected to oscillate with 50% probability into a B_s^0 meson, equal numbers of right-sign and of wrong-sign $\Xi^{\mp} - \ell^{\pm}$ pairs are expected.
  If the lepton comes from a non-strange $\bar{B}$ semileptonic decay, the $\Xi^{\mp}$ are less energetic because they have to be produced further down the hadronization chain. The contributions to right-sign and wrong-sign pairs should also be rather symmetric in this case (Fig. 3.c, d).
- The lepton originates from a charmed hadron decay: if the charmed hadron is produced in a B hadron cascade decay the previously quoted mechanisms have to be considered but the sign of the lepton is reversed and its transverse momentum relative to the jet axis will be usually smaller.
  If the charmed hadron comes from the fragmentation of a primary charm quark, in case of D_s semileptonic decays, there will be a contribution to wrong-sign $\Xi^{\mp} - \ell^{\pm}$ pairs only.
- Contribution from fake leptons: because of the quark content of the $\Xi^{\mp}$ it will be more probable to get a $\Xi^{\mp}$ accompanied by a kaon or a pion of opposite charge which can be identified as a muon. An excess of background is then expected in wrong-sign $\Xi^{\mp} - \mu^{\pm}$ pairs (Fig. 3.e).

From the above list it appears that all mechanisms in which the $\Xi^{\mp}$ is produced in the jet hadronization and is accompanied by a lepton emitted at large transverse momentum contribute in a similar way to right-sign and to wrong-sign $\Xi^{\mp} - \ell^{\pm}$ pairs with an excess expected in the second category.

6 Properties of the channel $\Xi_b \to \Xi^- \ \ell^- \ \bar{\nu}_l \ X$

Using a large sample of simulated events (section 7), the distributions of several kinematic variables are plotted in Fig. 4 for $\Xi_b \to \Xi^- \ \ell^- \ \bar{\nu}_l \ X$ and for all other mechanisms in which a $\Xi^{\mp}$ and a lepton, each with a momentum larger than 2 GeV/c, are produced in the same hemisphere. Each hadronic event is divided in two hemispheres by the plane normal to the thrust axis which contains the beam interaction point. The accepted ranges for the variation of these variables have been displayed in Fig. 4. The simulation includes a detailed modelling of the detector behaviour and these events have been analyzed using the same reconstruction algorithms as applied to the data [9].

- A Ξ^- produced from a Ξ_c decay secondary to a B-baryon benefits from the large fraction of the beam energy taken by the B-baryon and is usually faster than baryons coming from the fragmentation of the remaining light quark-antiquark system. This is shown in Fig. 4.a, where the lack of events below 2 GeV/c comes from a cut applied at simulation. $\Xi^{\mp}$ with a momentum larger than 3 GeV/c have been selected.
- The transverse momentum of the lepton, relative to the jet axis, has a distribution which extends to larger values than the corresponding distributions from other lepton sources such as B hadron cascade or direct charm semileptonic decays (Fig. 4.b).

Events with a lepton having a transverse momentum larger than 1 GeV/c have been kept.

- The mass of the $\Xi^{\mp} - \ell$ system is largely between 2 and 4.5 GeV/c^2. Combining a $\Xi^{\mp}$ with a lepton from another jet, the $\Xi^{\mp} - \ell$ mass can be large, while combinations of a $\Xi^{\mp}$ and a lepton from charm decays or those involving a $\Xi^{\mp}$ from hadronization can produce values below 2 GeV/c^2 (Fig. 4.c). Events with a $\Xi^{\mp} - \ell$ mass between 2 and 4.5 GeV/c^2 have been retained.
- Finally, if the B-baryon has a lifetime not very different from the other B states, the $\Xi^{\mp}$ and the lepton will originate from secondary vertices (usually not distinguishable from each other because of the very short Ξ_c^0 lifetime) which can be at a few millimeters from the main vertex of the event and in the jet direction. By selecting events with a decay distance larger than 1 mm, the signal is enhanced (Fig. 4.d).

7 Evidence for a signal in right-sign $\Xi^{\mp} - \ell^{\mp}$ pairs

The analysis has been performed in two steps. Evidence for Ξ_b baryon production has been obtained by evaluating the probability that a simulation which does not contain any B-baryon, reproduces the data. For this purpose, it has been investigated if the simulation gives a correct description of $\Xi - \ell$ pair production in kinematical regions where the effect of B-baryon decays is marginal and then the same comparison has been made in regions enriched in B-baryon decays. Finally the Ξ_b baryon production rate has been measured.

Three samples of simulated events have been analyzed. In the first sample, equivalent to 48 million hadronic Z^0 decays, each event contains at least one genuine $\Xi - \mu$ pair, the momenta of these two particles being greater than 2 GeV/c and with the lepton originating from a heavy flavour decay. This sample has been used to determine the contributions from the different production mechanisms to the $\Xi - \ell$ final state. The selection criteria described in section 6 have been applied to right-sign and wrong-sign $\Xi - \mu$ pairs separately. The results are summarized in Table 2.

	$\Xi^{\mp} - \mu^{\mp}$	$\Xi^{\mp} - \mu^{\pm}$
$P_{\Xi} > 3GeV/c$ and $2 < M_{\Xi\mu} < 4.5GeV/c^2$	3.9 ± 0.4	3.8 ± 0.4
and $P_T^{\mu} > 1GeV/c$	2.7 ± 0.3	1.9 ± 0.3
and Flight($\Xi\mu$) > 1mm	1.5 ± 0.2	0.4 ± 0.1

Table 2: Expected numbers of events in 1.7 million hadronic Z^0 decays, using the "HT" algorithm to reconstruct the $\Xi^{\mp}$ hyperon. Each event contains at least one genuine $\Xi^{\mp}$ and one genuine muon in the same hemisphere, there is no contribution from fake leptons in the quoted numbers.

The table 2 shows an excess of right-sign $\Xi^{\mp} - \ell^{\mp}$ pairs with a lepton emitted at large transverse momentum and with a positive decay distance greater than 1 mm. The analysis outlined in section 5 and including a detailed simulation of the physics, the

detector and the reconstruction algorithms shows that this excess comes from B-baryon semileptonic decays.

In the second sample, equivalent to 2.8 million hadronic Z^0 decays, all quark flavours have been generated; this sample has been used to study the contribution to lepton candidates from misidentified hadrons.

Finally, a sample equivalent to 2.3 million hadronic Z^0 decays has been used to study the level of the combinatorial background under the $\Xi^{\mp}$ mass peak obtained with the "HT" algorithm.

After having normalized the simulated events to the same number of hadronic Z^0 decays collected from 1991 to 1993, the number of $\Xi - \ell$ candidates found in the simulation and in the data have been compared in a region where the contribution from B baryons is expected to be negligible relative to other processes. For this purpose, wrong-sign $\Xi^{\mp} - \ell^{\pm}$ pairs have been used which satisfy P_{Ξ} greater than 3 GeV/c and M($\Xi - \ell$) between 2 and 4.5 GeV/c^2: no cut was applied to the lepton transverse momentum and the $\Xi^{\mp}$ hyperon was reconstructed by either of the "HT" and "$\Lambda\pi$" algorithms. Fig. 5.b, d give the $\Lambda\pi$ mass distributions obtained. In the simulation, because of the use of a dedicated sample of events, there is no combinatorial background under the $\Xi^{\mp}$ mass peak. The numbers of $\Xi^{\mp}$ candidates are shown in Table 3. In the data, the numbers of candidates have been determined by fitting a Gaussian distribution to account for the signal and a linear distribution for the background. The central value and width of the Gaussian are determined from the data themselves, through a larger $\Xi^{\mp}$ sample of similar energies.

$\Xi^{\mp} - \ell^{\pm}$	"$\Lambda\pi$"	"HT"
Data	29.2 ± 7.2	6.2 ± 3.4
Simulation (total)	29.8 ± 2.9	7.6 ± 1.0
Detailed contributions:		
Non B-baryons, genuine lepton	14.1 ± 0.8	4.1 ± 0.3
Non B-baryons, fake lepton	12.7 ± 2.8	3.0 ± 1.0
B-baryons	3.0 ± 0.4	0.5 ± 0.1

Table 3: Numbers of wrong-sign $\Xi^{\mp} - \ell^{\pm}$ pairs measured in data and in the simulation with the two $\Xi^{\mp}$ reconstruction algorithms.

The numbers of $\Xi^{\mp}$ in wrong-sign pairs agree in data and in the simulation. The relative error of the ratio between the two values, which is ± 27 %, will be taken as a measurement of the systematic uncertainty on the absolute normalization of all processes other than B-baryon decays present in the simulation contributing to the $\Xi - \ell$ final state.

In this comparison, the "$\Lambda\pi$" algorithm has been used because of its higher efficiency. The same value for the systematic uncertainty has been used for the "HT" algorithm because it was shown in section 4 that the relative efficiency of the two methods was reproduced by the simulation.

Fig. 5.a and c show the $\Lambda - \pi$ mass distribution for right-sign $\Xi^{\mp} - \ell^{\mp}$ pairs; an excess of candidates is observed in the data compared to the simulation. A comparison is given in table 4.

To check if this excess can be attributed to B-baryon decays, selection criteria have been applied to isolate samples of events in which the expected contribution from B-baryons is not marginal but even dominates, according to the arguments developed in sections 5 and 6. Only $\Xi^{\mp}$ reconstructed with the "HT" algorithm have been considered because of the reduced combinatorial background under the $\Xi^{\mp}$ mass peak and because the $\Xi^{\mp} - \ell$ vertex can be accurately defined.

$\Xi^{\mp} - \ell^{\mp}$	"$\Lambda\pi$"	"HT"
Data	41.0 ± 7.0	$13. \pm 4.$
Simulation (total)	22.8 ± 1.6	6.3 ± 1.1
Detailed model contributions:		
Non B-baryons, genuine lepton	10.9 ± 0.7	2.5 ± 0.3
Non B-baryons, fake lepton	6.3 ± 1.4	2.5 ± 1.0
B-baryons	5.6 ± 0.4	1.3 ± 0.3

Table 4: Numbers of right-sign $\Xi^{\mp} - \ell^{\mp}$ pairs measured in data and in the Monte Carlo simulation with the two $\Xi^{\mp}$ reconstruction algorithms.

$\Xi^{\mp}$ reconstructed using the "HT" algorithm and accompanied by a same sign lepton of transverse momentum larger than 1 GeV/c (Fig. 6) are in excess with respect to events from the simulation which contain no contribution from B-baryon decays. The results are summarized in Table 5 using the cuts described in section 6.

The measured values for wrong-sign $\Xi^{\mp} - \ell^{\pm}$ pairs are compatible with the expectations from the simulation. In this charge configuration the effect from B-baryons decays is expected to be small. The probabilities shown in Table 5 that the observed signals in right-sign $\Xi^{\mp} - \ell^{\mp}$ pairs be explained by statistical fluctuations of the expected numbers of events from all contributing mechanisms, without B-baryon decays have been evaluated using the following expression:

$$\mathcal{P}_{\mu_0}(\geq N) \;=\; \sum_{n=N}^{\infty} \int_0^{\infty} \frac{e^{-\frac{(\mu-\mu_0)^2}{2\sigma_0^2}}}{\sqrt{2\pi\sigma_0^2}} \times \frac{\mu^n e^{-\mu}}{n!}\, d\mu \qquad (4)$$

where N is the measured number of events in data, μ_0 is the expected number of events from the Monte Carlo simulation without contribution from B-baryons, and σ_0 is the uncertainty on μ_0 which corresponds to the sum of the statistical, the normalization (27%, see section 7.1) and the combinatorial background uncertainties added in quadrature.

	Right-sign pairs $\Xi^{\mp} - \ell^{\mp}$		Wrong-sign pairs $\Xi^{\mp} - \ell^{\pm}$	
Selection criteria	Data	M.C.	Data	M.C.
$P_{\Xi} > 3$ GeV/c $2 < M_{\Xi-\ell} < 4.5\ GeV/c^2$ $P_T^l > 1\ GeV/c$	10	NB $= 1.8 \pm 0.5$ Bckg. $= 0.24 \pm 0.14$ (B $= 1.80 \pm 0.22$) $\mathcal{P}_{3.6}(\geq 10) = 2.\%$	3	NB $= 3.2 \pm 1.2$ Bckg. $= 0.4 \pm 0.2$ (B $= 0.40 \pm 0.12$)
$P_{\Xi} > 3$ GeV/c $2 < M_{\Xi-\ell} < 4.5$ GeV/c^2 $P_T^l > 1\ GeV/c$ Flight$(\Xi - \ell) > 1$mm	7	NB $= 0.8 \pm 0.3$ Bckg. $= 0.10 \pm 0.09$ (B $= 1.20 \pm 0.17$) $\mathcal{P}_{1.1}(\geq 7) = 0.05\%$	1	NB $= 0.40 \pm 0.14$ Bckg. $= 0.30 \pm 0.15$ (B $= 0.12 \pm 0.07$)

Table 5 : Comparison between the numbers of right-sign and wrong-sign $\Xi - \ell$ pairs measured in data and expected from the simulation. The numbers of simulated events originating from B*-baryon semileptonic decays (B) and from all other sources (NB) have been quoted separately. The evaluation of the combinatorial background (Bckg) under the $\Xi^{\mp}$ mass peak is also given.*

To be independent of the details of the simulation and as the contribution from non B-baryon decays is expected to be larger in wrong-sign pairs, on quite general grounds (see section 5.2), μ_0 has been evaluated by taking the greater of the estimates in right-sign and wrong-sign pairs for the signal and the combinatorial background.

Thus we find that the $\Xi^{\mp}$ signals observed in the right-sign sample have less than 5×10^{-4} probability to be explained by a fluctuation of non-B baryon semileptonic decays.

A display of one candidate observed in the right-sign sample is given in Fig. 7. The $\Xi^{\mp}$ trajectory reconstructed by the "HT" algorithm has a large offset with respect to the primary vertex and the distance between the $\Xi - \ell$ vertex and the primary vertex, in the plane transverse to the beam direction, is 3 mm which corresponds to 9 times the measurement accuracy.

8 Ξ_b baryon production rate

The contribution from B-baryon semileptonic decays to the production rate of $\Xi - \ell$ pairs has been evaluated by subtracting the expected contribution from non B-baryon sources from the number of $\Xi^{\mp}$ candidates observed in data and comparing the result with the number of events expected from the simulation for Ξ_b and Λ_b semileptonic decays. Systematic uncertainties are calculated by estimating the capability of the simulation to account for the different contributions to $\Xi - \ell$ pairs of non B-baryon origin and by evaluating the experimental acceptance for the $\Xi^{\mp}$ and the lepton produced in a B-baryon direct semileptonic decay. The former contribution has been measured using the data in section 7.1. The latter is known with an accuracy of 10%, depending mainly on the understanding of the detector acceptance for $\Xi^{\mp}$ decays (section 4).

Results obtained with the two algorithms have been combined, keeping events reconstructed with the "HT" algorithm and adding those selected only with the "$\Lambda\pi$" method (Fig. 8). The observed numbers of $\Xi^{\mp}$ hyperons and the expected contributions from the different sources are given in Table 6.

Wrong-sign $\Xi^{\mp} - \ell^{\pm}$ pairs have not been included in the final measurement.

The absolute production rate of B-baryons decaying to the $\Xi^{\mp} - \ell^{\mp}$ final state is:

$$\mathcal{P}(b \to \text{B-baryon}) \times \text{BR}(\text{B-baryon} \to \Xi^{-}\ell^{-}X) \quad = \quad (5.9 \pm 2.1 \pm 1.0) \times 10^{-4} \ . \tag{5}$$

	$\Xi^{\mp} - \ell^{\mp}$	$\Xi^{\mp} - \ell^{\pm}$
Data	28.4 ± 6.1	15.2 ± 5.2
Simulation (total)	15.3 ± 1.5	13.9 ± 1.8
Simulation (components)		
Non B-baryon, genuine lepton	6.7 ± 0.5	7.0 ± 0.5
Non B-baryon, fake lepton	2.5 ± 1.3	4.6 ± 1.7
B-baryon	6.1 ± 0.5	2.3 ± 0.4

Table 6 : Numbers of $\Xi^{\mp} - \ell$ candidates measured in data and expected from the Monte Carlo simulation. The values for B*-baryon decays correspond to the probabilities of 7.8% and 1% to have, respectively, a Λ_b or a Ξ_b baryon in a b jet. Events have been selected as described in the text.*

This value is significantly lower than the rate of Λ_b baryon production, measured by LEP experiments [16] using the $\Lambda - l$ final state:

$$\mathcal{P}(b \to \Lambda_b) \times \mathrm{BR}(\Lambda_b \to \Lambda\ l^-\ X) \ = \ (3.2 \pm 0.3 \pm 0.8) \times 10^{-3}\ . \tag{6}$$

Assuming that the Λ_b production rate in a b quark jet is equal to (10 ± 5)% [17], the corresponding probability for a Ξ_b baryon to be produced can be expressed using (1), (2) and (5) as a function of still unmeasured branching fractions:

$$\begin{aligned} \mathcal{P}(b \to \Xi_b)(\%) \ &= \ (3.5 \pm 1.2 \pm 0.6 \ - \ (0.6 \pm 0.3) \times \mathrm{BR}(\Lambda_c \to \Xi^- X)(\%)) \\ &\times \ \frac{17.}{\mathrm{BR}_{(\Xi_c \to \Xi^- X)(\%)}} \ \times \ \frac{10.}{\mathrm{BR}_{(\Xi_b \to \Xi_c \ell^- \bar{\nu}_l X)(\%)}}\ . \end{aligned} \tag{7}$$

This corresponds to an excess of $3.3 \pm 1.2 \pm 0.6$ times the Monte Carlo expectations in which $P(b \to \Xi_b) \ = \ 1\%$ (section 5.1). To explain the measured excess of right-sign $\Xi^\mp - \ell^\mp$ pairs by Λ_b decays alone, the inclusive branching fraction $\mathrm{BR}(\Lambda_c \to \Xi^- X)$ would have to be of order 10^{-2}, a value which is unlikely considering the arguments developed in section 5.1. If, instead, this quantity is of order 10^{-3}, as expected, the $\Xi^\mp \ - \ \ell^\mp$ selected events originate mainly from Ξ_b baryon semileptonic decays.

9 Measurement of the lifetime of the Ξ_b baryon

The 10 candidates containing a right-sign $\Xi^\mp - \ell^\mp$ pair, selected by the "HT" algorithm and with the lepton transverse momentum larger than 1 GeV/c but without any cut on the $\Xi - \ell$ flight distance, have been used to measure the lifetime of Ξ_b baryonic states.

The proper time of the parent B hadron is measured in the following way.

The $\Xi^\mp$ track is reconstructed inside the VD and combined with the lepton trajectory to obtain the position of a secondary vertex. The decay distance between the primary and the secondary vertex has been measured in the plane transverse to the beam direction and computed in space using the angle of the momentum of the $\Xi - \ell$ system relative to the beam axis. This distance is positive if the secondary vertex is found beyond the primary vertex in the direction of the $\Xi - \ell$ momentum. The accuracy on the flight distance of the B-baryon, as obtained from the simulation, is $280 \pm 70\ \mu m$.

The Ξ_b baryon momentum is obtained, with a relative accuracy of (17 ± 3)%, from the measured momentum of the $\Xi - \ell$ system and using the Monte Carlo simulation to get the parameters of the correlation between these two quantities:

$$\mathrm{P}(\Xi_b) \ = \ \frac{\mathrm{P}_{(\Xi - \ell)}}{\mathrm{a}_0 \ + \ \mathrm{a}_1 \times \mathrm{P}_{(\Xi - \ell)}}\ ,$$

with $\mathrm{a}_0 \ = \ 0.30 \pm 0.05$ and $\mathrm{a}_1 \ = \ 0.019 \pm 0.003\ (GeV/c)^{-1}$.

An unbinned maximum likelihood method was used to fit the proper time distribution. The proper time probability distribution for the signal is an exponential convoluted with a Gaussian to account for the smearing in the Ξ_b baryon energy and decay distance measurements. The proper time probability distribution for the background has two components, a Gaussian and an exponential, whose parameters have been obtained using simulated events. In a sample of B-baryons, generated with 1.6 ps lifetime, the fitted lifetime was:

$$\tau(\mathrm{B - baryon} \to \Xi^- \ell^- X) \ = \ 1.4 \pm 0.3\ \mathrm{ps}\ ,$$

in agreement with the generated value.

The fitted lifetime for the data is (Fig. 9.):

$$\tau(\Xi_b) \;=\; 1.5^{+0.7}_{-0.4}(stat.) \pm 0.3(syst.) \text{ ps} \;.$$

where the systematic uncertainty corresponds to the statistical accuracy of the comparison between the generated and reconstructed lifetimes of the Ξ_b baryon from the simulated events. The other systematic errors, coming from the uncertainties on the fraction of background events, on the modelling of the B energy reconstruction and on the mass of Ξ_b baryonic states, are much smaller.

10 Conclusions

An algorithm which tracks charged $\Xi^{\mp}$ through the DELPHI Vertex Detector has been developed. It allows measurement of these particles to be performed with a very small combinatorial background and precise measurement of their decays vertices.

Events with a lepton with transverse momentum greater than 1 GeV/c and with a secondary $\Xi - \ell$ vertex displaced by more than 1 mm relative to the primary vertex, in the direction of the $\Xi - \ell$ system, have been selected. An excess of right-sign pairs has been measured, with a probability of 5×10^{-4} of being explained by mechanisms other than B-baryon decays. It has been checked that the Monte Carlo simulation correctly reproduced the number of $\Xi - \ell$ pairs in kinematical regions where the expected contribution from B-baryon decays is marginal.

From the number of right-sign pairs, obtained with two algorithms described in this paper, the production rate has been measured to be:

$$\mathcal{P}(b \to \text{B} - \text{baryon}) \times \text{BR}(\text{B} - \text{baryon} \to \Xi^- \; \ell^- \; X) \;=\; (5.9 \pm 2.1 \pm 1.0) \times 10^{-4} \;,$$

per lepton species, averaged over electrons and muons and assuming that the two channels have an equal contribution.

The contribution from Λ_b semileptonic decays followed by the $\Lambda_c \to \Xi^- K^+ \pi^+$ transition can account only for 6% of the observed signal.

The lifetime has been measured using a subsample of $\Xi^{\mp} \; - \; \ell^{\mp}$ events and found to be:

$$\tau(\Xi_b) \;=\; 1.5^{+0.7}_{-0.4} \pm 0.3 \text{ ps} \;.$$

Acknowledgements

It has been a pleasure to discuss this analysis with I. Bigi during his stay at CERN in 1994. We are greatly indebted to our technical collaborators and to the funding agencies for their support in building and operating the DELPHI detector, and to the members of the CERN-SL Division for the excellent performance of the LEP collider.

References

[1] A. Martin, Phys. Lett. B103 (1981) 51.

[2] D. Buskulic et al. (ALEPH Collaboration), Phys. lett. B294 (1992) 145.
P. Abreu et al. (DELPHI Collaboration), Phys. Lett. B289 (1992) 199.
P.D. Acton et al. (OPAL Collaboration), Phys. Lett. B295 (1992) 357.

[3] D. Decamp et al. (ALEPH Collaboration), Phys. Lett. B278 (1992) 209.
P.D. Acton et al. (OPAL Collaboration), Phys. Lett. B281 (1992) 394.
P. Abreu et al. (DELPHI Collaboration), Phys. Lett. B311 (1993) 379.

[4] P. Aarnio et al. (DELPHI Collaboration), Nucl. Instr. and Meth. A303 (1991) 233.

[5] N. Bingefors et al. (DELPHI Collaboration), Nucl. Instr. and Meth. A328 (1993) 447.

[6] P. Vincent "Mesure des rapports d'embranchement semileptoniques et de la contribution baryonique dans les désintégrations du quark b.", Thesis, LYCEN T 94-16, Lyon (1994).

[7] P. Abreu et al. (DELPHI Collaboration), Phys. Lett. B332 (1994) 488.

[8] T. Sjöstrand et al., Comp. Phys. Comm. 39 (1986) 347.

[9] DELSIM Reference Manual, DELPHI 87-98 PROG 100, Geneva, 1989.

[10] P.D Acton et al. (OPAL Collaboration), Phys. Lett. B291 (1992) 503.

[11] Review of Particle Properties, Particle Data Group, Phys. Rev. D50 (1994) 1173.

[12] B. Anderson et al. Phys. Scr. 32 (1985) 544.

[13] H. Albrecht et al. (ARGUS Collaboration), Phys. Lett. B247 (1990) 121.

[14] P. Avery et al. (CLEO Collaboration), Phys. Rev. Lett. 71 (1993) 2391.

[15] G. Crawford et al. (CLEO Collaboration), Phys. Rev. D45 (1992) 752.

[16] D. Buskulic et al. (ALEPH Collaboration), Phys. Lett. B294 (1993) 145.
OPAL Collaboration, contribution to the International Conference on High Energy Physics, Glasgow 1994, ref. GLS0534.
DELPHI Collaboration, contribution to the International Conference on High Energy Physics, Glasgow 1994, ref. GLS0162.

[17] S. Plaszczynski "Etude de la production des hypérons à LEP (DELPHI) et recherche de baryons beaux étranges." Thesis, LAL 94-17, Orsay (1994).

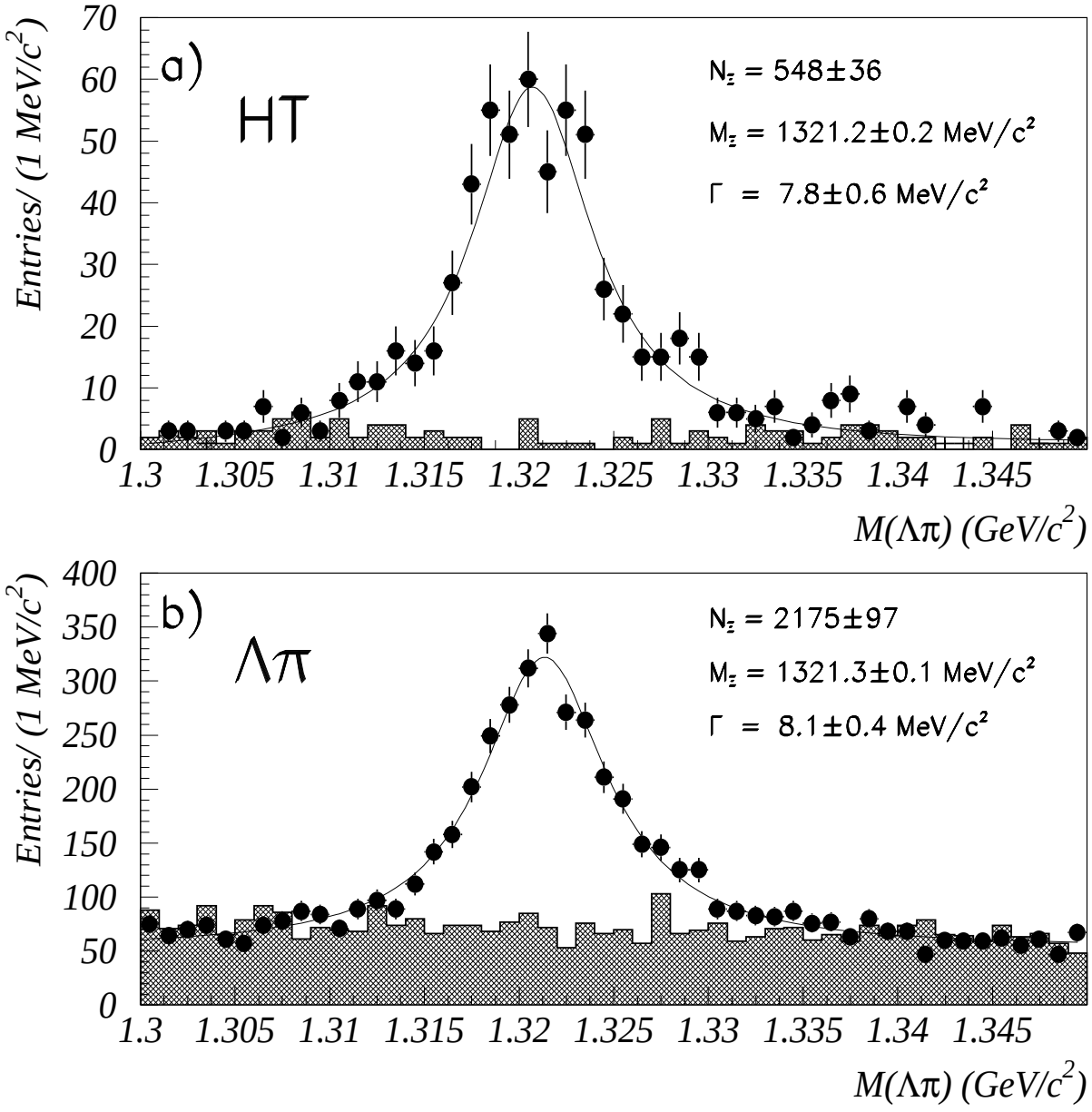

Figure 1: $\Lambda\pi$ mass distributions for events reconstructed with the "Hyperon tracking" (a) and "$\Lambda\pi$" (b) algorithms. The shaded histograms correspond to wrong-sign combinations. The curves have been obtained by fitting a Breit-Wigner distribution to account for the signal and a first order polynomial for the background. The numbers of $\Xi^{\mp}$ candidates have been evaluated inside an interval of ± 10 MeV/c^2 centered on the nominal $\Xi^{\mp}$ mass.

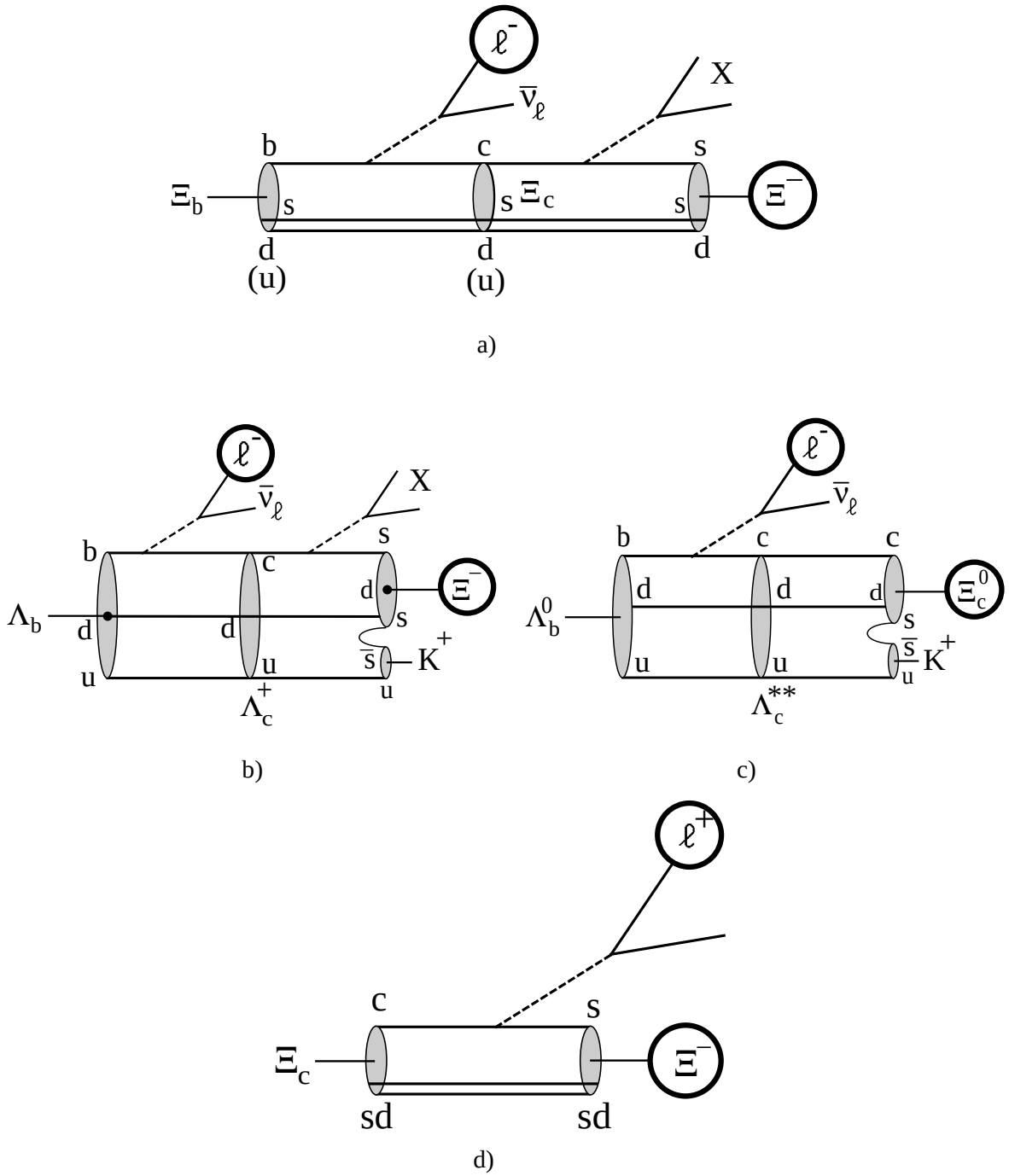

Figure 2: Schematic description of processes contributing to the production of $\Xi^{\mp} - \ell$ pairs in which the $\Xi^{\mp}$ originates from heavy flavour decays: (a) direct semileptonic decays of Ξ_b baryonic states; (b) direct semileptonic decays of a Λ_b with production of a $\Xi_c KX$ hadronic system; (c) direct semileptonic decays of a Λ_b in which the produced Λ_c^+ decays into ΞX; (d) direct semileptonic decays of Ξ_c states.

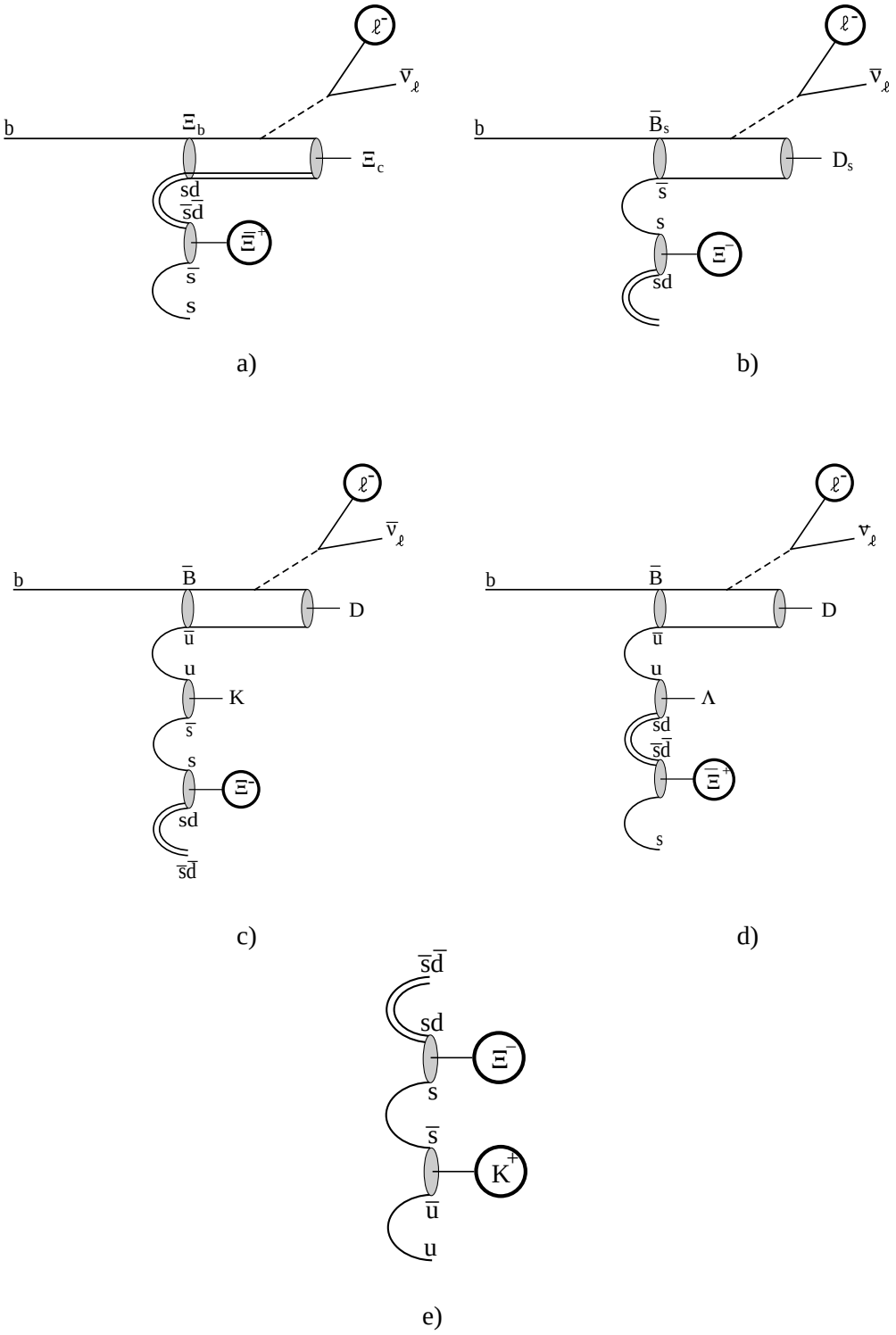

Figure 3: Schematic description of processes contributing to the production of $\Xi^{\mp}-\ell$ pairs in which the $\Xi^{\mp}$ originates from the primary vertex of the event. (a) Direct semileptonic decays of Ξ_b baryonic states, with a $\Xi^{\mp}$ produced during the hadronization of the jet. The correlation with the lepton is of wrong-sign. (b) Direct semileptonic decays of B_s^0. Because of $\mathrm{B}_s^0 - \bar{\mathrm{B}}_s^0$ oscillation there will be as many right-sign and wrong-sign $\Xi^{\mp} - \ell$ pairs. (c, d) Direct semileptonic decays of $\bar{\mathrm{B}}_d^0$ or B^- mesons. (e) Example of a possible contribution from fake leptons, a misidentified K^+ in this case.

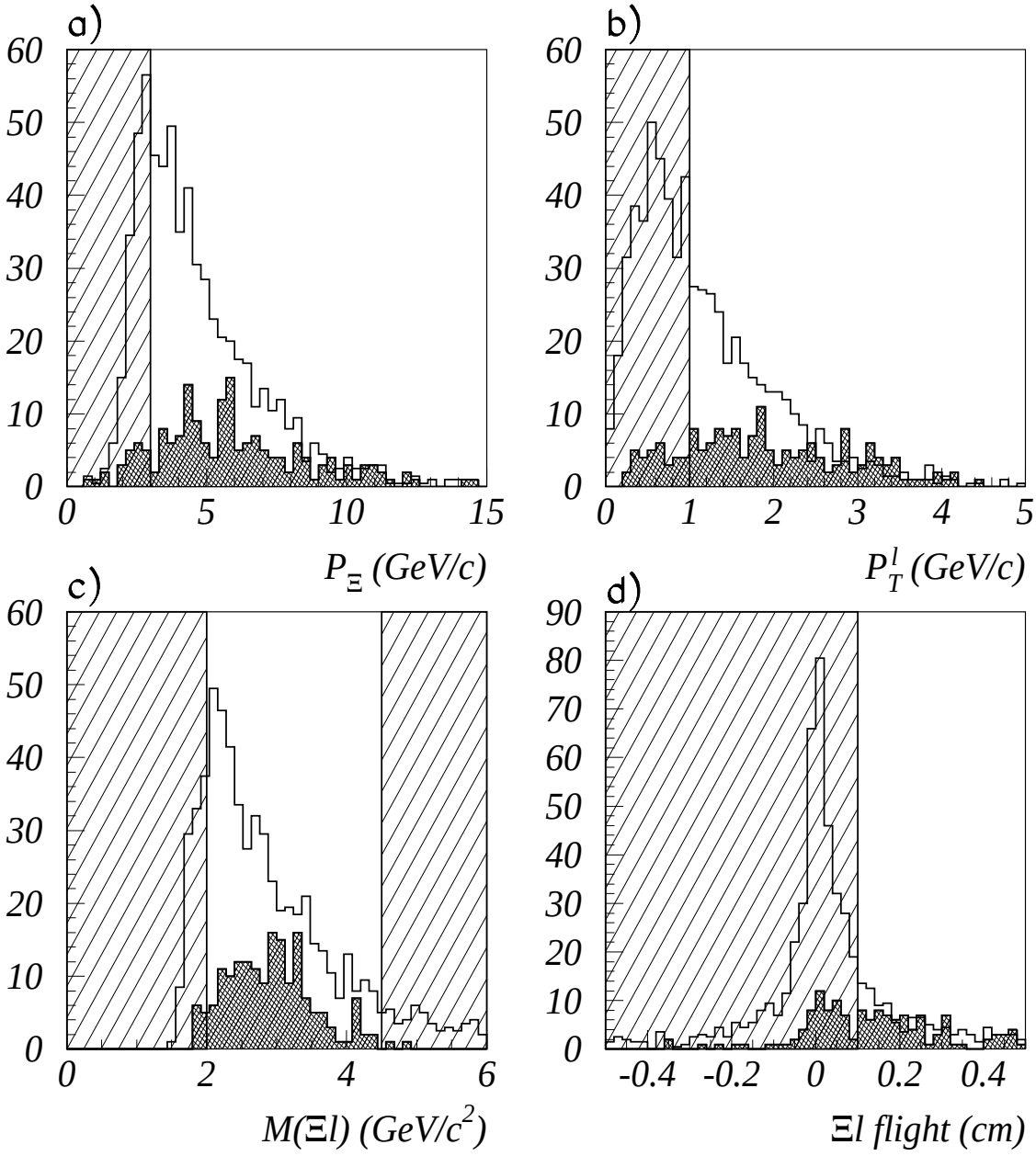

Figure 4: Distributions of the variables, from simulated events, to select semileptonic decays of B-baryons. (a) $\Xi^{\mp}$ momentum distribution. (b) Lepton transverse momentum distribution. (c) $\Xi - \ell$ mass distribution. (d) Algebraic distance between the $\Xi - \ell$ vertex and the primary vertex measured in the direction of the momentum of the $\Xi - \ell$ system. Events originating from a B-baryon direct semileptonic decay are shown in cross-hatched histograms; other sources are displayed in un-hatched histograms. Regions rejected by the applied selection cuts are shown inside single-hatched areas.

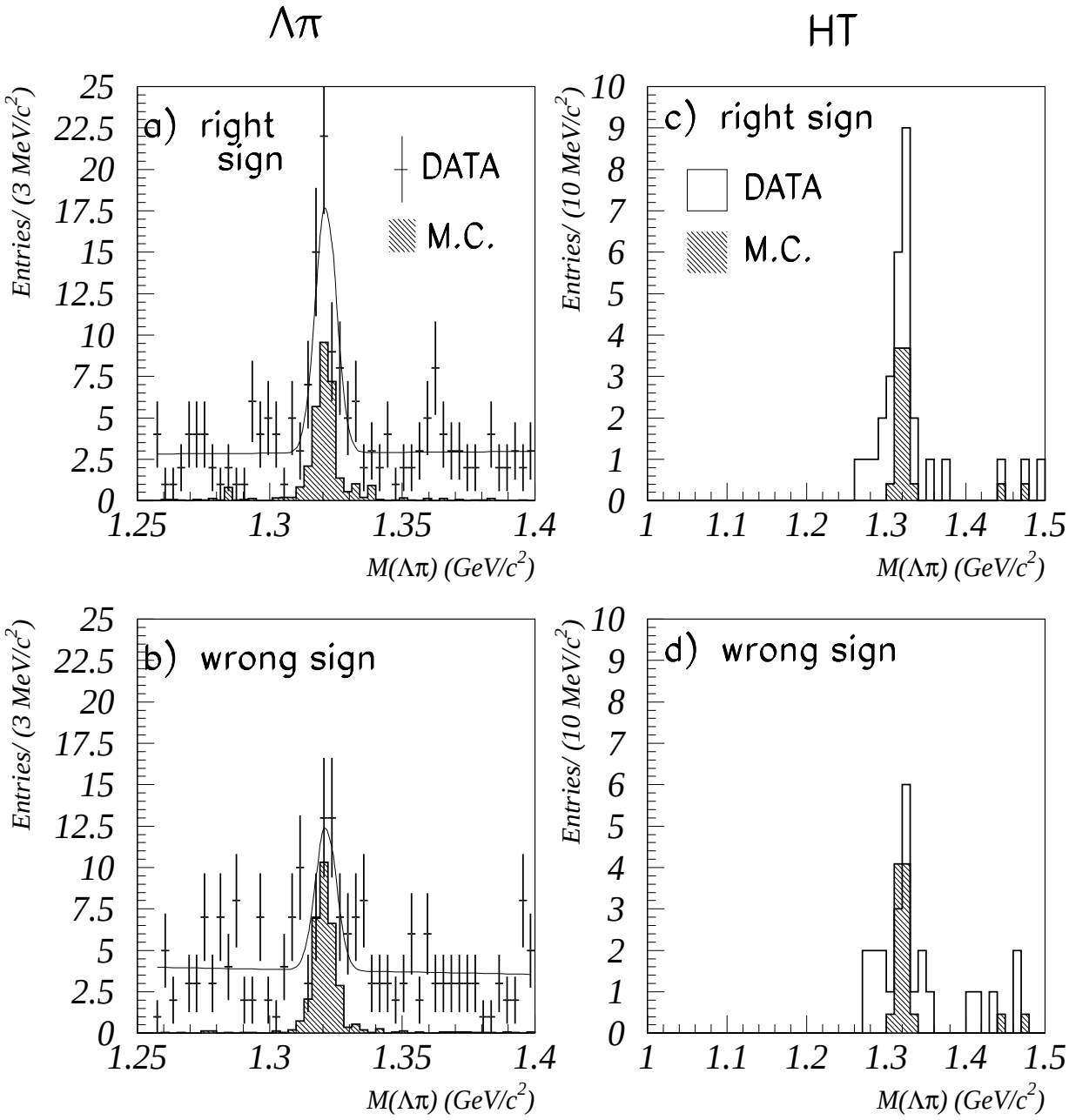

Figure 5: Comparison between measured and expected numbers of right-sign and wrong-sign $\Xi^{\mp} - \ell$ pairs. The hatched histograms represent the Monte-Carlo events, which include only the contribution from Λ_b and Ξ_b semileptonic decays but not the combinatorial background. The fitted curves are the sum of a first order polynomial distribution to describe the combinatorial background and of a Gaussian distribution of fixed width and central values to account for the signal.

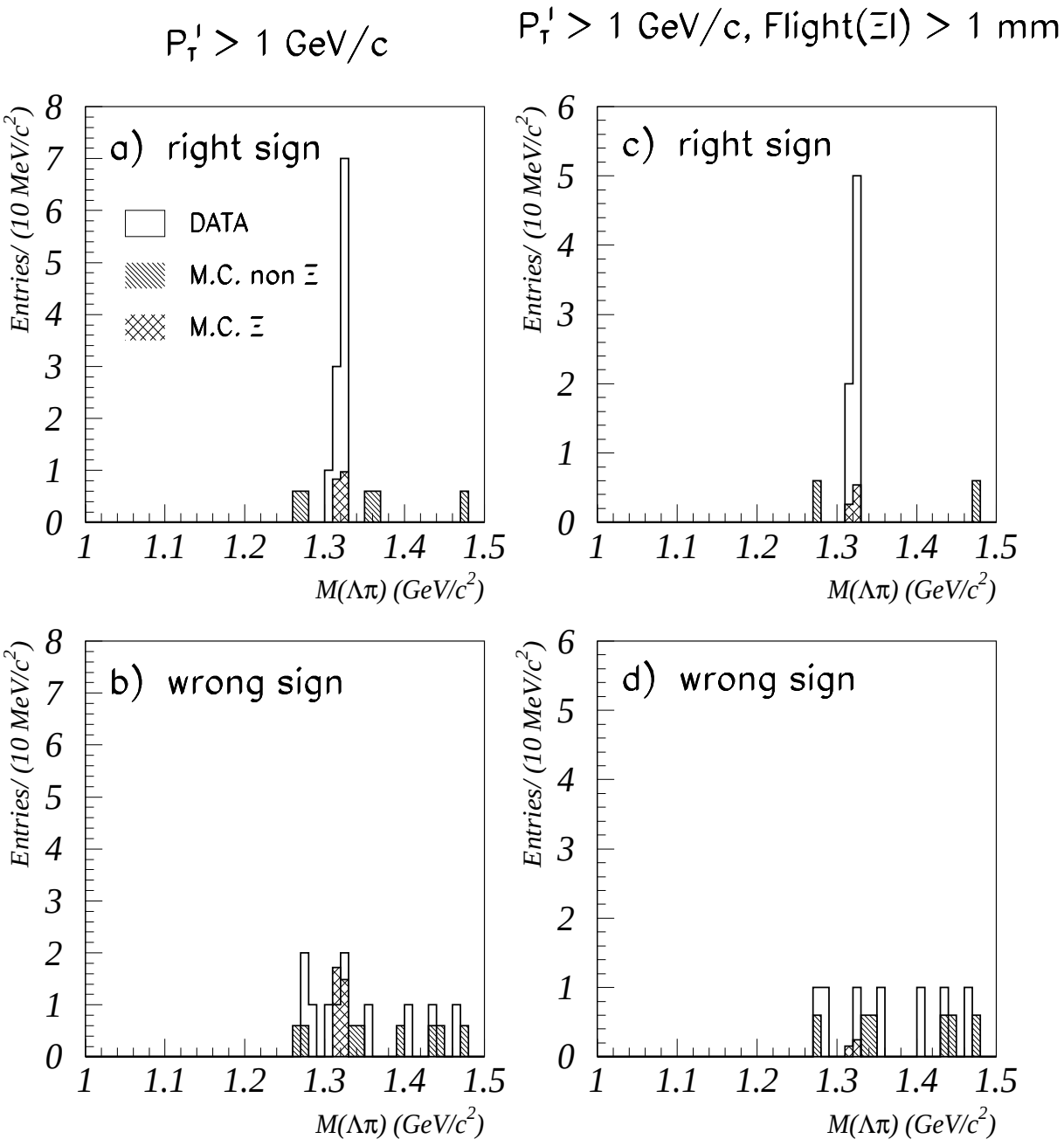

Figure 6: $\Lambda\pi$ mass distributions obtained with the "HT" algorithm for right-sign and wrong-sign $\Xi^{\mp} - \ell$ pairs. (a, b) The lepton transverse momentum is larger than 1 GeV/c (c, d) In addition, the distance between the primary and the $\Xi^{\mp} - \ell$ vertex, measured in a plane transverse to the beam axis, in the direction of the jet containing the $\Xi^{\mp}$ hyperon, has to be larger than 1mm.

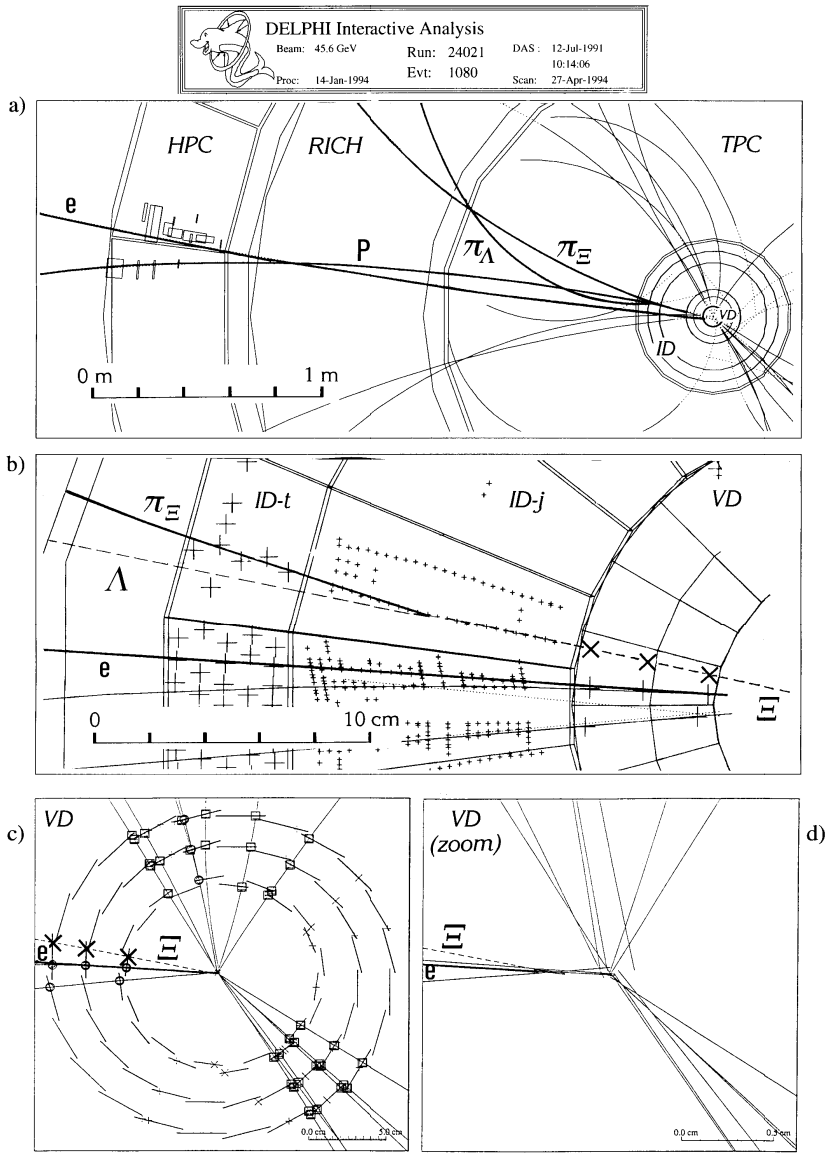

Figure 7: Displays of one Ξ_b candidate. (a) Display of the charged particle tracks showing the hyperon decay products and the energy deposited by the electron candidate in the electromagnetic calorimeter (HPC). (b) Closer view inside the detectors situated between the beam pipe and the entrance of the TPC. A kink corresponding to the decay of the $\Xi^\mp$ in the jet chamber part of the Inner Detector (ID-j) is visible. (c) Display of the three layers of the VD. The three hits created by the $\Xi^\mp$ track are shown as dark crosses. (d) Enlarged view close to the beam interaction point. The ellipses centered on the primary and secondary vertex positions correspond to 3 times the measurement error.

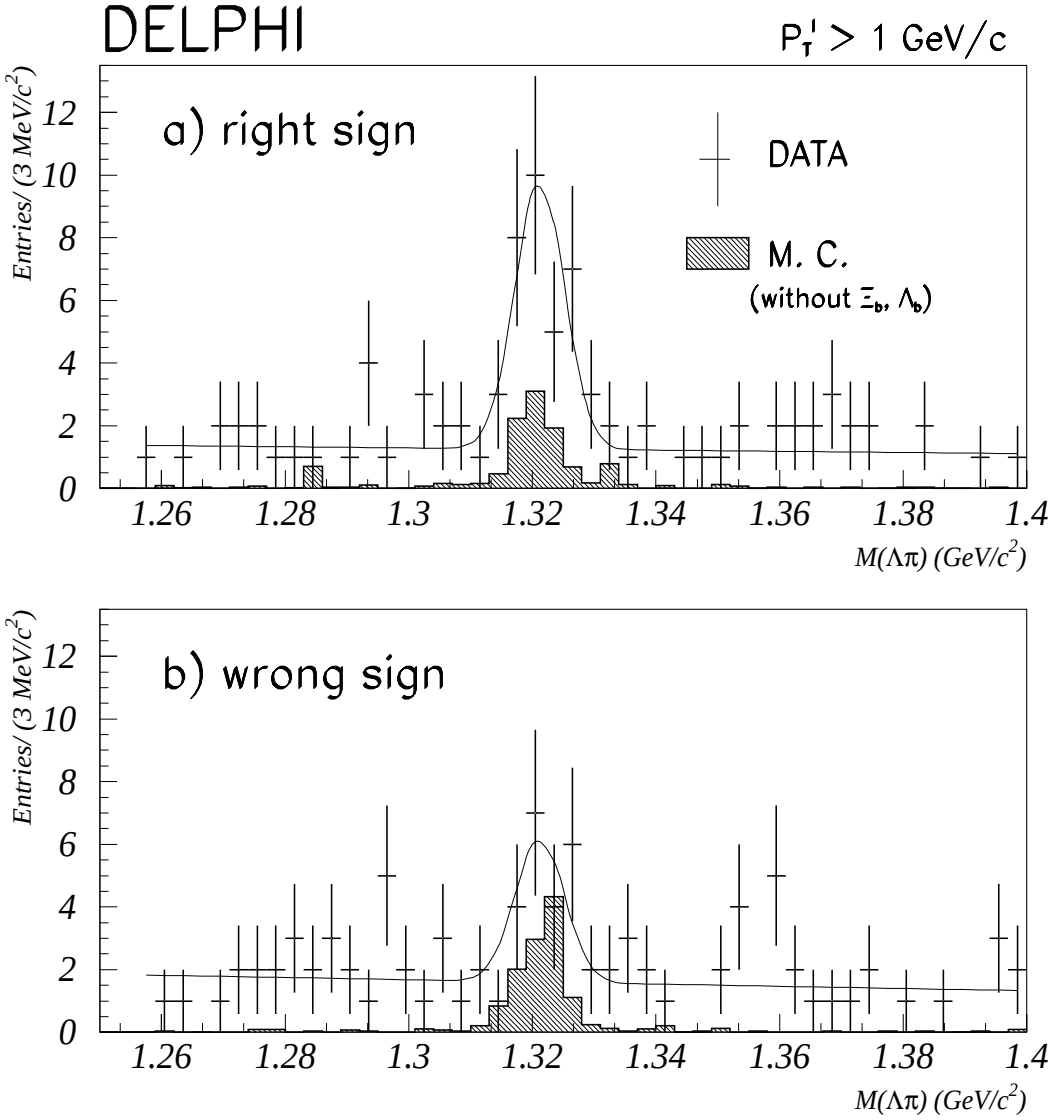

Figure 8: Comparison between measured and expected numbers of right-sign and wrong-sign $\Xi^{\mp} - \ell$ pairs when the contribution from B-baryon decays is not included in the Monte Carlo simulation. The distributions contain all the different candidates reconstructed with at least one of the two algorithms: "HT" and "$\Lambda\pi$". The Monte Carlo expectations, normalized to the total number of hadronic events analyzed in the data, are given in hatched histograms. The simulation is not expected to account for the combinatorial background under the signal.

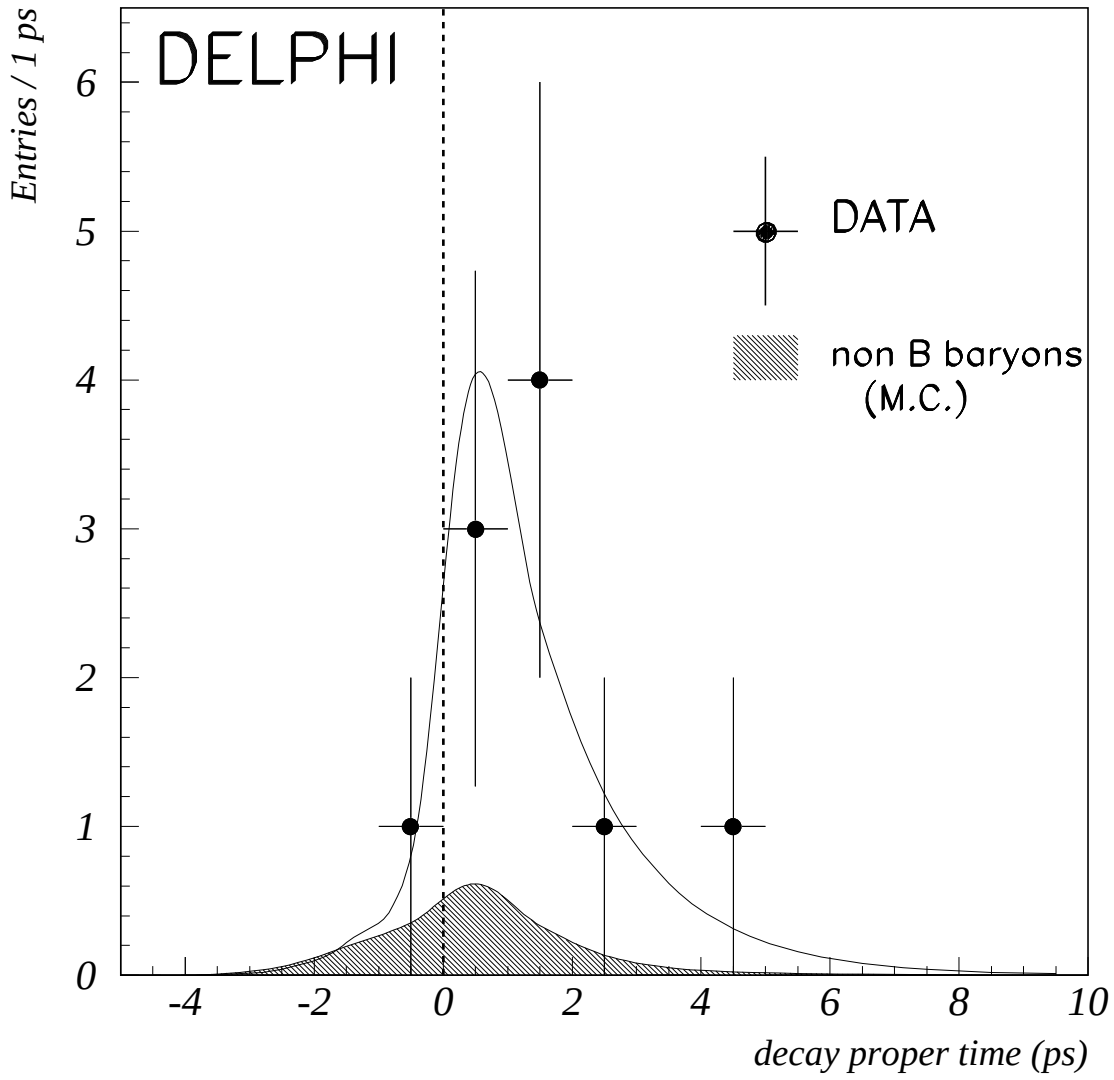

Figure 9: Proper time distribution of the 10 right-sign $\Xi^{\mp} - \ell^{\mp}$ events selected with $P_T^l > 1$ GeV/c using the "HT" algorithm. The shaded area corresponding to the expected distribution for non B-baryon events has been obtained from the Monte Carlo simulation (rate and shape).